SCREENING OF FDA-APPROVED DRUG LIBRARY FOR COMBINATORIAL TREATMENT OF PANCREATIC CANCER CELLS WITH ONCOLYTIC VESICULAR STOMATITIS VIRUS

by

Molly Cate Holbrook

A thesis submitted to the faculty of
The University of North Carolina at Charlotte
in partial fulfillment of the requirements
for the degree of Master of Science in
Biology

Charlotte

2021

Approved by:

_____

Dr. Valery Grdzelishvili

_____

Dr. Adam Reitzel

_____

Dr. Andrew Truman

ABSTRACT

MOLLY CATE HOLBROOK. Vesicular Stomatitis Virus Against Pancreatic Ductal Adenocarcinoma. (Under the direction of DR. VALERY GRDZELISHVILI)

Pancreatic ductal adenocarcinoma (PDAC) is a devastating malignancy with poor prognosis and a dismal survival rate, expected to become the second leading cause of cancer-related deaths in the United States. Oncolytic virus (OV) is an anticancer approach that utilizes replication-competent viruses to preferentially infect and kill tumor cells. Vesicular stomatitis virus (VSV), one such OV, is already in several phase I clinical trials against different malignancies. VSV-based recombinant viruses are effective OVs against a majority of tested PDAC cell lines. However, some PDAC cell lines are resistant to VSV. Upregulated type I IFN signaling and constitutive expression of a subset of interferon-simulated genes (ISGs) play a major role in such resistance, while other mechanisms, such as inefficient viral attachment and resistance to VSV-mediated apoptosis, also play a role in some PDACs. Several alternative approaches have been shown to break the resistance of PDACs to VSV without compromising VSV oncoselectivity, including (i) combinations of VSV with JAK1/2 inhibitors (such as ruxolitinib); (ii) triple combinations of VSV with ruxolitinib and polycations improving both VSV replication and attachment; (iii) combinations of VSV with chemotherapeutic drugs (such as paclitaxel) arresting cells in the G2/M phase; (iv) arming VSV with p53 transgenes; (v) directed evolution approach producing more effective OVs.

In this study, we investigated a library of Food and Drug Administration (FDA) approved pharmaceutical drugs to evaluate whether drug treatment impacted viral

replication, to determine if any drugs could sensitize cancer cells to viral infection by a library screening. The DiscoveryProbe FDA-Approved Drug Library of 2018 which contains 1,496 FDA-approved drugs, and the screening was conducted in five different cell lines, including four phenotypically distinct PDAC cell lines with varying degrees of permissiveness to viral infection and one non-malignant cell line to evaluate oncoselectivity of VSV-drug combinations. Two independent screenings identified several promising FDA-approved drugs stimulating VSV replication to varying degrees across the range of PDAC cell lines, which did not exhibit cytotoxicity in non-malignant cells. Interestingly, several commonly used pancreatic cancer chemotherapeutics were seemingly ineffective or even inhibited VSV replication in all five cell lines. From the complete table, we selected our candidate drug, R788 Disodium (fostamatinib), for further evaluation of the mechanism of activity. Fostamatinib is tyrosine kinase inhibitor often used for the treatment of chronic immune thrombocytopenia (ITP). Syk plays a large role in signal transduction and inflammatory propagation and immune activation, and inhibition could have a negative effect on many interrelated pathways. Our study is critical to the development of rational chemovirotherapy approaches to enhance oncolytic virotherapy efficacy and broaden the spectrum of pancreatic cancers that can be successfully treated.

DEDICATION

To my mother, Perri, my siblings, Rachel and Jacob,

and my grandparents, Jewell and Charles Holbrook.

ACKNOWLEDGMENTS

This work was made possible by the mentorship of Dr. Valery Grdzelishvili, thank you for your guidance and the opportunity to work in your lab. I would like to thank my committee members, Dr. Adam Reitzel, and Dr. Andrew Truman for their important feedback and guidance. Thank you to members of the Grdzelishvili lab, Dakota Goad, Sara Seegers, Isha Wilson, Abdul Hajjar, and Jessica Miller for your technical assistance, moral support, and friendship throughout my graduate career. Thank you to the following laboratories for kindly providing reagents for this project: Jack Rose (Yale University) for VSV-ΔM51; Michael Hollingsworth (University of Nebraska Medical Center) for SUIT-2 cells; Pinku Mukherjee (University of North Carolina at Charlotte) for MIA PaCa-2.

I want to thank UNCC's department of Biology for funding and technical support. This research was supported by V.Z.G's grants, 1R15CA195463-01A1 and 1R15CA238864-01 from the National Cancer Institute, National Institutes of Health (Bethesda, Maryland, USA).

TABLE OF CONTENTS

LIST OF FIGURES

LIST OF ABBREVIATIONS

Ds – double stranded

G – glycoprotein

GFP – green fluorescent protein

IFN – interferon

L – large polymerase protein

LDLR – low-density lipoprotein receptor

M – matrix protein

ΔM51 – deletion of the methionine at position 51

MOI – multiplicity of infection

N – nucleocapsid protein

NNS – nonsegmented negative-strand

OV – oncolytic virus

PDAC – pancreatic ductal adenocarcinoma

PS – phosphatidylserine

ss – single stranded

STAT – signal transducer and activator of transcription

VSV – vesicular stomatitis virus

WT – wild type

rWT – recombinant wild type

HIF – hypoxia inducible factor

ISG – interferon stimulated genes

IGF – insulin-like growth factor

Jak – janus kinase

IRDS – interferon-related DNA damage resistance signature

p1 – position 1

SeV – sendai virus

dCK – deoxycytidine kinase

dFdC – difluorodeoxycitidine

dFdCDP – difluorodeoxycitidine diphosphate

dFdCTP – difluorodeoxycitidine triphosphate

rdrp – RNA-dependent RNA polymerase

ITP – immune thrombocytopenia

Syk – spleen tyrosine kinase

CHAPTER 1: INTRODUCTION

1.1 Background

Viruses represent the most abundant biological entities on earth and are characterized as submicroscopic, obligate intracellular parasites minimally comprised of nucleic acid contained within a protective protein coat (Koonin, 2010; Perlmutter and Hagan, 2015). While viruses have gained notoriety from pathogenic behavior, they also provide many benefits, especially in biological research. Viruses are excellent models for genetic research and are critical to areas such as vaccine development and gene therapy, as vectors for gene, bacteriophage, and cancer therapy (Draper and Heeney, 2010; Felt and Grdzelishvili, 2017; Thomas et al., 2003; Lin et al., 2017; Russell et al., 2012; Verma and Weitzman, 2005).

1.1.2 Pancreatic Ductal Adenocarcinoma

Pancreatic ductal adenocarcinoma (PDAC) is the most common form of abdominal malignancy, and represents a critical challenge to healthcare, as it is characterized as having an especially high mortality rate(Holbrook et al., 2021). Despite being only the 13th most common type of cancer, PDAC is the fourth-leading cause of cancer-related deaths and is predicted to become the second-leading cause of cancer-related death by 2030, as incidence increases while rates of survivorship remain stagnant due to late diagnosis and limited treatment options (Aier et al., 2019). PDAC is a highly invasive malignancy, which forms a dense stromal desmoplastic reaction, characterized by a dramatic increase in the proliferation of alpha-smooth muscle actin-positive fibroblasts and an increased production of many extracellular matrix components

(Kamisawa, 2016). Family history, diabetes, and smoking are the most well-established risk factors for developing pancreatic cancer.

As we have discussed previously, KRAS, CDKN2A, TP53, and SMAD4 serve as driver genes for PDAC development, and the vast majority of patients with fully established pancreatic cancer carry genetic defects in at least one of these genes (Bressy et al., 2019). Mutations in KRAS are present in 90% of PDAC tumors, 95% of PDAC tumors have mutations in CDKN2A (encodes p16), 50–75% in TP53, and SMAD4 (DPC4) is lost in approximately 50% of PDAC tumors (Siegel, 2020). Mutated KRAS oncogene leads to an abnormal, constitutively active, Ras protein. This results in aberrant activation of pathways responsible for survival and proliferation (Buscail et al., 2020). Inactivation of the tumor suppressor gene CDKN2A results in the loss of p16, a protein that serves as a regulator of the G1-S checkpoint of the cell cycle. Abnormalities in TP53 prevent it from acting as a tumor suppressor protein, including its important role as a regulator of DNA-damage check-points. Furthermore, many p53 mutants acquire devastating gain-of-function onco-genic activities, actually promoting cell survival, proliferation, invasion, migration, chemoresistance, and chronic inflammation. SMAD4 (DPC4) is related to the TGF-β signaling pathway, but some mutations result in abnormal signaling by TGF-β, a transforming growth factor receptor on the cell surface which can further increase the risk of cancer development by increasing the rate of cell growth and replication. In addition, germline mutations within BRCA2, BRCA1, ATM, and other genes were frequently identified in PDACs as inherited traits increasing susceptibility to PDAC development later in life (Salo-Mullen et al., 2015; Shindo et al., 2017). These

genes, especially when identified as being comorbid, are correlated with a significantly higher metastatic burden (Cicenas et al., 2017; Wong et al., 2020; Yachida et al., 2012).

The primary treatments for PDAC include surgical resection, chemotherapy, radiotherapy, and palliative care (McGuigan et al., 2018). Surgical resection still retains the greatest chance of success for potentially curing PDAC, however late-stage diagnosis due to ambiguous symptoms often results in tumors that are too-far progressed for surgery alone. Less than 25% of patients that present with PDAC are eligible for surgical resection, and 5-year survivorship of completely resected patients is approximately 37% (Siegel, 2020).

In addition, even in patients where surgical resection was performed with either preparatory or subsequent adjuvant chemotherapy, there is a high rate of recurrence, and up to 80% of patients with recurrent PDAC will relapse with local and/or distant disease, which is associated with mortality within 2 years from diagnosis. Recent advances in the understanding of the molecular biology, diagnosis, and staging of PDAC will hopefully lead to greater progress in the development of novel treatment approaches for PDAC patients. One such approach is oncolytic virus (OV) therapy, which utilizes replication-competent viruses to preferentially infect, replicate in, and kill cancer cells. In this review, we will discuss current advances with OV therapy for PDAC, with a special focus on vesicular stomatitis virus (VSV), the major interest of our laboratory. For comprehensive reviews of gene therapy for pancreatic cancer (unlike oncolytic virotherapy, gene therapy is typically based on replication-defective viral vectors for transgene delivery), we refer to these excellent papers (Rouanet et al., 2017; Sato-Dahlman and Yamamoto, 2018).

1.1.3 Major Challenges with Current PDAC Treatments

Since 1997, gemcitabine-based chemotherapy has been the standard first-line treatment for patients with unresectable locally advanced, or metastatic pancreatic cancer with a median survival rate of 4.4–5.6 months, especially when patients are not healthy enough for combination therapies (Springfeld et al., 2019). Gemcitabine (dFdC) is an analog of deoxycytidine and a pro-drug that, once transported into the cell, must be phosphorylated by cellular deoxycytidine kinase to gemcitabine diphosphate (dFdCDP) and gemcitabine triphosphate (dFdCTP), both of which can inhibit processes required for DNA synthesis. Other commonly used chemotherapies for pancreatic cancer include 5-fluorouracil (5-FU), oxaliplatin, albumin-bound paclitaxel, capecitabine, cisplatin, irinotecan, and docetaxel (Lambert and Banks, 2019; Turpin et al., 2020). Although several gemcitabine-based combination treatments exist, most have not considerably improved survival. While some combinatorial chemotherapy treatments, such as gemcitabine with erlotinib, have demonstrated potential for longer patient survival, the majority of patients eventually experience tumor progression due to the development of resistance, and therefore novel therapies are required, especially those that do not rely solely on chemotherapeutic drugs (Parekh et al., 2017; Perri et al., 2020).

The mechanisms of de novo or inherent resistance of PDACs to chemo- or radio-therapeutics are not well understood. Several factors have been demonstrated to contribute to such resistance, including (i) multiple factors associated with the nature of the PDAC tumor microenvironment (TME) (Dauer et al., 2017; Kleeff et al., 2007); (ii) nucleoside transporters or/and nucleoside enzymes affecting drug uptake and metabolism (Adamska et al., 2018); (iii) hypoxia-inducible factor-1 alpha (HIF-1α) regulated glucose

metabolism (Akakura et al., 2001); (iv) stromal-derived Insulin-like Growth Factors (IGFs) (Ireland et al., 2016); (v) abnormal expression of tumor-associated mucin proteins (Trehoux et al., 2015); (vi) IFN-related DNA-damage resistance signature (IRDS) of some tumors (Weichselbaum et al., 2008). The understanding of chemo-resistance of PDACs to chemotherapy is very important, as at least some of these mechanisms could be also contributing to the resistance of PDACs to OV therapy.

The success of any treatment for PDAC is further complicated by the TME of PDAC, which is characterized by dense stroma comprised of abundant fibroblasts, hypoxia, and sparse vasculature. Moreover, the infiltration of tumor-promoting immune cells mediates immune evasion and promotes tumor progression. The stroma surrounding the tumor is primarily composed of pancreatic stellate cells (PSCs) which are activated by secreted factors such as TNFα, TGF-β, and interleukins 1, 2, 10, and themselves secrete mucins, collagen, fibronectin, and laminin in addition to some other factors, forming a thick extracellular matrix (ECM). This composition generates an in-credibly dense physical barrier, to both host immune cells and potential therapeutics while also increasing interstitial pressure, which, when combined with sparse vasculature, forms a hypoxic environment, further inhibiting immune cells in terms of recruitment and effectiveness. PI3K/Akt, a key downstream mediator of many receptor tyrosine kinase signaling pathways involved in cell proliferation, migration, and inhibition of apoptosis, is phosphorylated under hypoxic conditions, along with MAPK (Erk), which regulates cell proliferation in response to various growth factors, which have been associated with resistance to gemcitabine (Daisuke Uchida 1, 2014; Kohei Horioka 1, 2016). The limits on antitumor immune cell recruitment also leads to T-cell exhaustion resulting in loss of

cytotoxic effector function and further limits appropriate immune responses. SDF-1α/CXCR4 signaling-induced activation of the intracellular FAK-AKT and ERK1/2 signaling pathways and a subsequent IL-6 autocrine loop in cancer cells can further increase chemoresistance (Chad A Barnes, 2019).

The low expression of nucleoside transporters (NT) and inactivity of nucleoside enzymes (NE) both affect the activity of gemcitabine. Low expression of a nucleoside transporter hENT1 restricts the uptake of gemcitabine, preventing its incorporation into the DNA of replicating cancer cells, and high expression of hENT1 is related to longer overall survival in pancreatic cancer patients (Giovannetti et al., 2006; Spratlin et al., 2004). The inactivation of deoxycytidine kinase (dCK), an enzyme responsible for the initial phosphorylation of gemcitabine, also mediates resistance. dCK is often inactivated in gemcitabine-resistant PDAC lines (Ohhashi et al., 2008), and knockdown of dCK has been shown to lead to the development of resistance (Saiki et al., 2012), while expression of a DCK transgene (along with uridine monophosphate kinase) sensitized pancreatic cancer cells to gemcitabine (Vernejoul et al., 2006).

Pancreatic cancers metabolize glucose at higher rates and show higher expression of HIF-1α positively correlated with gemcitabine resistance (Kasuya et al., 2011; Zhang et al., 2018). HIF-1α increases glucose uptake and metabolism in the cell and is stabilized by MUC1, a common biomarker for cancers including PDAC (Wang et al., 2020). Knockdown of HIF-1α in gemcitabine-resistant cells reduced tumor cell survival following gemcitabine treatment, and treatment with digoxin, and HIF-1α inhibitor, reduced glucose uptake and cell survival in cells treated with gemcitabine (Shukla et al., 2017). The increased glucose uptake under hypoxic conditions feeds into the glycolysis

pathway and increases biomass; however, the exact mechanisms by which HIF-1α reduces sensitivity to chemotherapeutics have yet to be determined.

In addition, stromal-derived IGFs activate the insulin/IGF1R survival signaling pathway, reducing responsiveness to chemotherapeutics (Mutgan et al., 2018). One proposed mechanism describes crosstalk between activated Insulin/IGF signaling pathways in PDAC. IGF-1 and IGF-1R, which are known to be abundantly expressed in the PDAC tissue, can stimulate β-cell proliferation and increase β-cell mass, increasing basal insulin production which may alter the trophic effects of the endocrine cells on the exocrine cells. Endocrine β-cells that express oncogenic K-ras can also be one potential progenitor for PDAC under chronic tissue inflammation (Gidekel Friedlander et al., 2009). This is further supported by evidence that demonstrates macrophages and myofibroblasts are the two major sources of IGFs within the pancreatic tumor microenvironment, and that chemoresistance is increased when cytotoxic agents increase M2-like macrophage infiltration (Ireland et al., 2016). For any novel therapies to be effective, they should be able to address most if not all of these challenges.

The structural composition of mucins produced by cells in certain cancers, such as breast and pancreatic cancers, has been suggested to limit immune cell recognition by blocking infiltration (Kalra and Campbell, 2007). Similarly, the dense mucin mesh prevents cellular uptake of chemotherapeutics like gemcitabine and 5-FU within the tumor. MUC1 and MUV4 are overexpressed and aberrantly glycosylated in the majority of pancreatic tumors (Nath et al., 2013). Kalra et al. demonstrated that the inhibition of mucin O-glycosylation enhanced the cytotoxic effects of 5-FU against human pancreatic cancer cell lines, but not against the mucin-deficient cell line [40]. They suggest that pre-

venting the formation of the mucin facilitates the diffusion of drugs across the compromised mucus layer, improving intracellular drug uptake and enhancing cytotoxic drug action.

Elevated MUC1 and MUC4 expression have also been correlated with greater degrees of resistance to gemcitabine (Dang, 2017). It was also demonstrated that gemcitabine-resistant cells had accentuated the non-oxidative branch of the pentose phosphate pathway activity and increased pyrimidine biosynthesis, conferring resistance by increased dCTP production. MUC1 and MUC4 overexpression was also shown to upregulate mdr genes in pancreatic cancer cells, including ABCC1, ABCC3, ABCC5, and ABCB1 genes (Bafna et al., 2009; Nath et al., 2013). MUC4 expression was shown to be conversely correlated with the expression of hCNT1 and hCNT3 transporters, preventing uptake of chemotherapeutic drugs like gemcitabine, and hCNT1 is upregulated when MUC4 is inhibited, resulting in increased drug sensitivity (Skrypek et al., 2013). Finally, MUC4-overexpressing CD18/HPAF-Src were not sensitive to gemcitabine, conferring resistance and survival advantages through erbB2-dependent and anti-apoptotic pathways (Mimeault et al., 2010). Altogether, mucins including MUC1 and MUC4 have been demonstrated to be highly overexpressed and aberrantly glycosylated in pancreatic cancer cells, conferring resistance to various chemotherapies and the downregulation of these oncoproteins may represent a promising therapeutic strategy for reversing chemoresistance and reducing tumor progression and mass.

Type I IFN signaling is upregulated in some tumors responding to chemotherapy and can have antitumor as well as pro-tumor effects. The expression of a type I IFN-related DNA-damage resistance signature (IRDS) was reported to correlate with

resistance to chemotherapy and radiotherapy in multiple cancer types. In breast cancer, the IRDS has been implicated in the development of chemoresistance, which may be another potential mechanism of resistance in PDACs as well (Weichselbaum et al., 2008). The STAT1/IFN pathway transmits a cytotoxic signal either in response to DNA damage or to IFNs, such as in the case of viral infection. Cells with an IRDS (+) profile show constitutive activation of the STAT1/IFN pathway.

Interestingly, this chronically activated state of the STAT1/IFN pathway may select against transmission of a cytotoxic signal, instead resulting in pro-survival signals mediated by STAT1 and other IRDS genes (Weichselbaum et al., 2008). In agreement with this mechanism, STAT1 is highly upregulated in many cancers, including PDAC, and protects SCC-61 cells from ionizing radiation-mediated death (Amorino et al., 2002). STAT1 may also induce resistance with other DNA damage-based treatments, such as gemcitabine, and may transduce survival/growth signals that enhance tumor survival under some conditions (Zeng et al., 2019). Sensitivity to DNA damage is coupled with sensitivity to IFNs such that selection for resistance to one may lead to resistance to the other (Khodarev et al., 2004), which could prove to be a problem with not only chemo- and radiotherapies, but OV treatments as well.

1.1.4 Oncolytic Virotherapy Overview

The oncolytic potential of viruses was first observed in the 19th century, as researchers found that naturally acquired infections could also lead to tumor regression in patients, and we have since found that many viruses exhibit an inherent preference for infecting, replicating in, and killing cancer cells. Naturally occurring or engineered viruses that exhibit this preference are now known as oncolytic viruses (OVs). However,

in the past we observed limited success with OV treatment due to inconsistent or unreliable oncoselectivity, the specificity for only malignant cells, and due to viral clearance in immunocompetent patients by the immune system before the virus was able decrease tumor growth (Kelly and Russell, 2007).

The oncoselectivity of most OVs, including VSV, is primarily a result of defective or reduced type I IFN responses in cancer cells (Balachandran and Barber, 2004; Barber, 2004; Lichty et al., 2004; Marozin et al., 2008; Marozin et al., 2010; Moussavi et al., 2010; Stojdl et al., 2000; Stojdl et al., 2003; Zhang et al., 2010), compared to non-malignant ("normal") cells. Many cancer cells down-regulate or lose antiviral signaling responses during oncogenesis, because the loss confers a growth advantage; these responses are generally unfavorable for tumor development as they are anti-proliferative, anti-angiogenic, and pro-apoptotic (Wang et al., 2011). Through the process of developing and improving OV, many viruses have been engineered to refine oncoselectivity by exploiting their susceptibility to innate immune responses (Ayala-Breton et al., 2013). Viruses have also been engineered to target distinctive biomarkers of malignant cells with higher specificity to further improve oncoselectivity (Freedman et al., 2018). Engineered OVs have had pre-clinical and clinical success with three OVs currently approved to be used in clinical settings for melanoma treatment.

1.1.5 VSV as an OV

VSV is a prototypic nonsegmented negative-strand (NNS), RNA virus from the family *Rhabdoviridae*. VSV typically infects mammals such as livestock, resulting in blistering stomatitis, or sores on the mouth and feet of infected individuals throughout regions of the Americas. VSV can naturally infect humans, however the symptoms are

usually much less severe (Tesh et al., 1969) and there is a distinct lack of pre-existing immunity in the human population because VSV is not typically a human pathogen (Felt and Grdzelishvili, 2017b; Hastie and Grdzelishvili, 2012b; Simovic et al., 2015). VSV is a well characterized virus widely used in studies involving gene therapy, vaccine development, and oncolytic virotherapy (Bukreyev et al., 2006; Ke et al., 2020). VSV is an enveloped, bullet shaped virus with an 11-kb genome encoding five proteins: nucleocapsid protein (N), phosphoprotein (P), matrix protein (M), glycoprotein (G), and large polymerase (L) (Gaddy and Lyles, 2007).

Wild-type (WT) VSV is sensitive to type I IFN mediated antiviral responses in most normal tissues, however WT VSV-M protein sufficiently inhibits type I IFN responses to allow viral replication in the central nervous system (CNS) (Clarke DK, 2007; Johnson JE et al., 2007). Thanks to a well-established reverse-genetics system available for VSV, a large number of safe VSV-based oncolytic viruses have been generated and tested in numerous studies (Felt et al., 2017; Hastie and Grdzelishvili, 2012b). Many of the most widely used oncolytic VSVs are recombinants carrying a deletion (ΔM51) or substitution (M51R) of methionine at amino acid (aa) residue 51 in VSV-M. These mutations attenuate VSV replication in normal cells by preventing WT VSV-M protein from inhibition the exonuclear transport of host mRNAs, including transcripts for virus-induced antiviral genes (Black and Lyles, 1992; Black et al., 1993; Coulon et al., 1990). As a result VSV M51 mutants have dramatically attenuated neurotoxicity but retain robust oncolytic abilities (Ahmed et al., 2003; Brown et al., 2009; Ebert et al., 2005; Kobbe et al., 2000; Stojdl et al., 2003; Trottier et al., 2007; Wollmann et al., 2010).

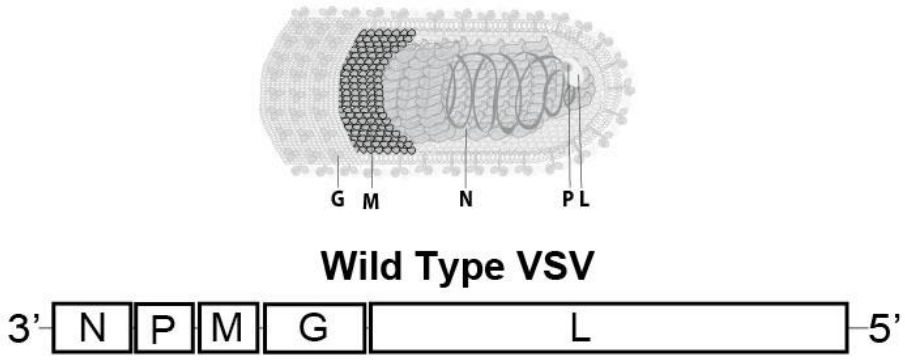

Figure 1: Wild type VSV virion structure and genome. VSV has a non-segmented negative sense RNA genome that encodes 5 proteins: N, P, M, G, L that assemble as an enveloped, bullet-shaped virion. Adapted from Hastie et.al.

As a result of the numerous preclinical studies demonstrating the effectiveness of different VSV recombinants as OVs (Felt and Grdzelishvili, 2017a; Hastie and Grdzelishvili, 2012a; Russell et al., 2012), VSV-hIFNbeta-NIS, encoding the human cytokine interferon beta (hIFNbeta) and the human thyroidal sodium-iodine symporter (NIS), is currently being tested in the United States in several phase I clinical trials against various malignancies (see details at ClinicalTrials.gov for trials NCT02923466, NCT03120624, and NCT03017820).

Despite these advances, many challenges exist regarding the use of VSV as an oncolytic virus in clinic. Not all tumors are susceptible or permissive to VSV (Felt et al., 2017; Hastie and Grdzelishvili, 2012b). Our previous studies showed that PDACs show a broad spectrum of susceptibility and permissibility to VSV based OVs, such as VSV-ΔM51. We previously identified several mechanisms of resistance to VSV-based therapy, such as residual or upregulated type I IFN antiviral activities (Cataldi et al., 2015; Hastie et al., 2016; Moerdyk-Schauwecker et al., 2013; Murphy et al., 2012a), inefficient

attachment of VSV to some PDACs (Felt and Grdzelishvili, 2017b), and resistance to virus-mediated induction of apoptosis (Felt et al., 2015).

Due to the nature of VSV's RNA genome, there is the potential for rapid mutation as the virus-encoded RNA-dependent RNA polymerase (RdRp) has lower fidelity than DNA polymerases and lacks proofreading activity (Steinhauer et al., 1992). Such spontaneous mutations could revert attenuated VSV back to a less oncoselective WT phenotype. For example, in the case of VSV-ΔM51 recombinants, secondary mutations in VSV-M could potentially restore M protein functions and reduce safety. VSV also has a small genome, and the addition of any transgenes typically attenuates viral replication as the added genetic information hinders speed of genome replication and attenuates transcription of downstream viral genes (Wertz et al., 2002). The spontaneous loss of a transgene, particularly if the transgene is the attenuating factor, is an undesirable possibility. In addition, single site mutations in beneficial transgenes could abrogate or alter function, resulting in an ineffective or potentially pathogenic activity. However, there is evidence that VSVs genome remains relatively stable in endemic regions and even with the insertion of large transgenes (Letchworth et al., 1999; Seegers et al., 2020).

VSV is able to infect a wide range of hosts and replicate in a wide range of cell types (Hastie et al., 2013b) due to ubiquitously expressed cell-surface receptors that can be used by the virus. The low-density lipoprotein receptor (LDLR) and other members of the LDLR family have been shown to serve as VSV receptors (Amirache et al., 2014; Ammayappan et al., 2013; Finkelshtein et al., 2013; Nikolic et al., 2018), and additional studies showed that other cell surface molecules, such as phosphatidylserine (Carneiro et al., 2006; Coil and Miller, 2004; Schlegel et al., 1983), sialoglycolipids (Schloemer and

Wagner, 1975), and heparan sulfate (Guibinga et al., 2002) could also play a role in VSV attachment to host cells. VSV-G is the viral protein responsible for attachment and entry into host cells through the interaction with the previously mentioned known receptors on the host cells surface. VSV-G contains 2 sites that are post translationally glycosylated which have been shown to play a role in cell infection depending on the cell line being infected however other non-specific interactions between the virus and host cell that alter the efficacy of VSV attachment to host cells (Hastie et al., 2013b). Treatment with polycations has been shown to improve VSV attachment to host cells most likely by decreasing electrostatic repulsion between the negatively charged viral envelope and the negatively charged cell membrane (Bailey et al., 1984; Conti et al., 1991).

After VSV attaches to a host cell via specific and non-specific interactions, VSV is endocytosed into the host cell. Fusion of the viral envelope with the endosomal membrane occurs when pH decreases in the endosomal vesicle resulting in a conformational shift in VSV-G that is responsible for the fusion of membranes. which in turn releases the viral nucleocapsid into cells cytoplasm. VSV has a negative sense RNA genome and its genome must first be transcribed to mRNA from which viral proteins can be synthesized and assembled with the replicated negative sense RNA viral genome. Once new progeny virions are assembled, they bud from the host cells plasma membrane which VSV-G has been incorporated into, which is where the new VSV virions gain their envelope. Host cell must be permissive and able to support each step of the virus replication cycle to result in infectious viral progeny and different cell lines result in differing amounts of virion production depending on their permissiveness to the viral infection.

Our previous studies demonstrated that VSV is effective against the majority of tested human pancreatic ductal adenocarcinoma (PDAC) cell lines, both *in vitro* and *in vivo*. However, we found that some PDAC cell lines are resistant to VSV infection, replication, and/or virus-mediated oncolysis. In this study, we investigated a library of Food and Drug Administration (FDA) approved pharmaceutical drugs to evaluate whether drug treatment impacted viral replication, to determine if any drugs could sensitize cancer cells to viral infection by a library screening.

1.1.6 Overview of Experimental Model Used to Study OV Therapy

Oncolytic virus (OV) therapy is a relatively novel anticancer approach. Effective OV therapy is dependent on the oncoselectivity of OVs—their ability to preferentially infect, replicate in and kill infected cancer cells without damaging nonmalignant ("normal") cells. The ideal OV therapy not only requires the direct lysis of cancer cells by the virus but also activates innate and adaptive anticancer immune responses (Russell L, 2019) (Figure 2).

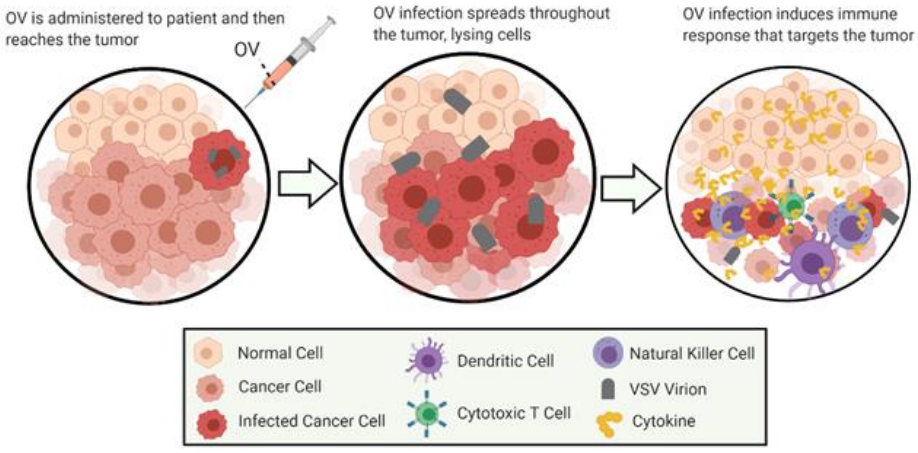

Figure 2. General Overview of Oncolytic Virotherapy. This figure demonstrates the general method of action for the treatment of cancer by oncolytic virotherapy using

Vesicular Stomatitis Virus (VSV) as the OV. The images depict the infection and oncolysis of malignant cells over time, followed by immunostimulation of cells invading the cleared area. This figure was made by Molly Holbrook using Biorender (Holbrook et al., 2021).

Preclinical PDAC models are critical for understanding the biology of PDAC, are platforms for developing novel strategies against PDAC, and are a necessary part of the drug development pipeline. There are several features of an ideal PDAC model system to develop clinically relevant OV therapy against PDAC: (1) the ability to test OV against different PDACs, characterized by various responsiveness to different therapies, including OV therapy; (2) the model should recapitulate a complex TME of PDACs; (3) tractability of the model, including the ability to trace both tumor cells and OV; (4) the ability to deliver OV systemically, as the PDAC are difficult to access; (5) the ability to detect and evaluate innate and adaptive immune responses against both tumor cells and OV. Unfortunately, there is no single PDAC model that successfully recapitulates all these critical features and challenges of the disease. However, there are numerous models for PDAC, each with unique advantages and disadvantages. Here, we will briefly review the advantages and disadvantages of various in vitro and in vivo models of PDAC and how they can contribute to the development of OV therapeutics.

Numerous human PDAC cell lines have been established and can be characterized by their distinctive genotypic and phenotypic variations, including their relative permissiveness or resistance to OV infection (Deer et al., 2010; Moerdyk-Schauwecker et al., 2013; Murphy et al., 2012b). Utilizing cell lines as a model system offers several advantages for studying PDAC, including easy propagation and indefinite growth. These

features represent a cost-effective and consistent model that can easily be used to study molecular mechanisms and biomarkers of resistance or permissiveness of PDAC cells to OVs (Deer et al., 2010; Moerdyk-Schauwecker et al., 2013). While cell line-based approaches represent quick, straightforward, and consistent models, several features reduce their clinical translatability. First, the homogeneous nature of cell line models fails to accurately represent the heterogeneous nature of typical in vivo tumors, including PDAC (Gillet et al., 2013).

Indeed, cell lines are under selection for mutations and phenotypes allowing growth advantage in a monolayer, however, the selection mechanisms in vivo are different (Froeling et al., 2010). In fact, established PDAC cell lines not only lose the heterogeneity present in the primary tumor, but the evolution of these cell lines to grow in culture may obscure genetic aberrations present in the primary tumor (Deer et al., 2010). Additionally, many PDAC cell lines are originated from metastasized disease, so the ability to study PDAC progression is severely limited. Secondly, cell lines cultured in a monolayer lack the important three-dimensional structure and function as seen in vivo (Froeling et al., 2010). Thirdly, the PDAC cell line model fails to represent the TME, which is understood to be a dynamic player in PDAC tumor progression (Froeling et al., 2010). Lastly, cultured cell lines lack selection pressure from the host adaptive immune system, thus leaving mutations necessary for evading host immunity underrepresented. The outcome of the OV therapy depends on the complex interaction between tumor cells, virus, and innate and adaptive immune systems of the host. One of the desirable outcomes of this interaction is OV-mediated stimulation of immune response against tumor cells. However, normal PDAC stromal cells can induce innate antiviral responses

against OV replicating in tumor cells, and adaptive immune response can prematurely clear virus infection instead of targeting tumor cells. Unfortunately, cell culture-based models cannot address these important issues.

Even given the disadvantages of the cell line model, it is a good starting proof-of-principle platform that has allowed our group to investigate mechanisms regarding responsiveness or resistance to OV therapy (Bressy et al., 2019; Cataldi et al., 2015; Felt et al., 2017; Felt et al., 2015; Hastie et al., 2013a; Hastie et al., 2016; Hastie et al., 2015; Moerdyk-Schauwecker et al., 2013; Murphy et al., 2012b; Seegers et al., 2020). For example, our group is interested in understanding why/how certain PDAC cell lines are more resistant to VSV infection than other PDAC cell lines (Moerdyk-Schauwecker et al., 2013). The cell line model in this aspect allows for reliable comparative measurements of virus replication, spread, and cell lysis. Additionally, the cell line model allows for relatively straightforward screening of both cellular and viral genes and proteins of interest. Cell line models allow for efficient virus tractability through reporter genes such as GFP (Torres et al., 2013). Additionally, cell culture-based systems allow innovative imaging approaches for single-cell real-time analysis of OV replication and efficacy in pancreatic cancer cells (Quillien et al., 2021).

1.1.7 Overview of the Current Progress in OV Therapy for PDAC

In 2015, the FDA approved Talimogene laherparepvec (T-VEC; Imlygic™), a genetically modified herpes simplex virus, to treat melanoma (Eissa et al., 2018). T-VEC is the first and still the only FDA-approved OV. However, numerous OVs are currently in preclinical studies and clinical trials for various malignancies, including PDAC. Additionally, gene therapy targets, such as oncogene knockdown, insertion of functional

tumor-suppressor genes, and expression of functional RNAs also demonstrate improved cancer-killing efficacy when combined with OV. One method uses adenoviruses and adeno-associated viruses to deliver apoptotic genes to tumor cells. Such gene therapy using Adenovirus subtype 5 mediates rat insulin promoter directed thymidine kinase (A-5-RIP-TK)/ganciclovir (GCV) gene therapy resulting in significantly enhanced cytotoxicity to both Panc1 and MiaPaCa2 pancreatic cancer cells in vitro (Monsurro et al., 2010). Another review explored the potential use of OV expressing functional p53 (Bressy et al., 2017). Another method would use OV to deliver siRNA transgenes for oncogenetic knockdown, such as ONYX-411-siRNA^{ras} expressing a mutant K-ras siRNA which significantly reduced K-ras mRNA expression at 48 h posttreatment and improved oncolytic activity (Zhang et al., 2006). The inclusion of an endostatin-angiostatin fusion gene in VVhEA also showed significant antitumor potency in vivo (Tysome et al., 2009).

There have been many experiments screening for more effective virotherapies within available libraries, and modulated viruses such as the adenovirus AdΔCAR-SYE has been shown to significantly suppress tumor growth, and complete regression of tumors was observed in vivo (Nishimoto et al., 2009). In addition, more efficient and tumor-specific targeting peptides and OV could be identified by using additional libraries, and modifications to existing OV based on these findings are also promising. Such modifications have been shown to be effective, with the adenoviruses VCN-01 variants ICOVIR-15K and ICOVIR-17 (Rodriguez-Garcia et al., 2015). As discussed previously, the ability of the OV to modulate the ECM was observed, as tumors treated with VCN-01 showed a dramatic decrease in the intratumoral HA content (Rodriguez-Garcia et al., 2015). Other adenoviral variants such as Ad5PTDf35(pp65) have also

demonstrated T-cell stimulation and dendritic cell (DC) modulation to increase efficient transduction within a human context (Yu et al., 2013).

Combinatorial treatments of chemotherapies, or chemovirotherapy, such as OV paired gemcitabine, have demonstrated improved oncolytic capabilities in vitro and in vivo than either treatment on their own. In vitro and in vivo studies showed that myxoma virus (MYXV) and gemcitabine therapies can be combined sequentially to improve the overall survival in intraperitoneal dissemination (IPD) models of pancreatic cancer (Wennier et al., 2012). The addition of chemotherapies to OV therapy using a combination of an oncolytic herpes simplex virus-1 mutant NV1066 with 5-FU increased viral replication up to 19-fold compared with cells treated with virus alone, and similar results were achieved by the addition of gemcitabine (Eisenberg et al., 2005). Similarly, oVV-Smac combined with gemcitabine greater cytotoxicity and potentiated apoptosis (Chen et al., 2019). H-1PV combined with cisplatin, vincristine or sunitinib induced effective immunostimulation via a pronounced DC maturation, better cytokine release and cytotoxic T-cell activation (Moehler et al., 2011). The addition of gene targets alongside chemovirotherapy has also shown greater cytotoxic efficiency, as with VV-ING4 in combination with gemcitabine (Wu et al., 2017). Even in cell lines that demonstrate resistance to viral infection, resistance can be broken with simultaneous treatments. Viruses like VSV rely on nonspecific interactions with the cell surface during the earliest stages of infections, and polycations have been shown to improve viral production and increase oncolysis by increasing the amount of virus interacting with cells during attachment (Felt et al., 2017). Additionally, the use of JAK inhibitors like ruxotinilib and IKK inhibitors like TPCA-1 have also been shown to increase viral

reproduction and oncolysis (Cataldi et al., 2015; Felt et al., 2017). Other potential combinatorial treatment regimens could include radiovirotherapy or chemoradiotherapy.

Some of these treatment methodologies are already being tested in clinical trials. Table 2 describes the OV currently being tested in clinical trials, and while some are still underway, OV including ONYX-15, AD5-yCD, and T-VEC are well-tolerated, and in some cases, biologically active, either alone or in combination chemovirotherapies (Chang et al., 2012; Hecht et al., 2003; Hirooka et al., 2018; Lee et al., 2020; Mahalingam et al., 2020; Mulvihill et al., 2001).

1.1.8 Understanding Molecular Mechanisms of Responsiveness and Resistance of PDACs to VSV-Based OV Therapy

VSV is a promising oncolytic virus against various malignancies, and it has several advantages as an OV (Felt and Grdzelishvili, 2017c; Hastie et al., 2013b; Hastie and Grdzelishvili, 2012b): (i) its basic biology and interaction with the host have been extensively studied. The oncoselectivity of VSV is mainly based on VSV's high sensitivity to Type I interferon (IFN) mediated antiviral responses (and therefore inability to replicate in healthy cells), while it can specifically infect and kill tumor response cells, most of which lack effective Type I IFN responses; (ii) although WT VSV can cause neurotoxicity in mice, nonhuman primates, several VSV recombinants, including VSV-ΔM51, have been generated which are not neurotropic but retain their OV activity; (iii) VSV has a broad tropism for different types of cancer cells (including PDACs), as its primary mode of entry into a host cell utilizes binding of the VSV-G protein to LDLR, which is ubiquitous, and VSV-G is also capable of using other common surface molecules for cell entry (Hastie et al., 2013b); (iv) there is no preexisting immunity

against VSV in most humans; (v) replication occurs in the cytoplasm without risk of host cell transformation; (vi) cellular uptake occurs rapidly; (vii) VSV has a small, easily manipulated genome, and novel VSV-based recombinant viruses can be easily engineered via reverse genetics to improve oncoselectivity, safety, oncotoxicity, and to work synergistically with host immunity and/or other therapies in a specific tumor environment (e.g., PDAC); (viii) as other members of the order *Mononegavirales*, and compared to positive-strand RNA viruses, VSV is less likely to mutate, and our recent study demonstrated long-term genetic stability of VSV recombinants carrying large transgenes (Seegers et al., 2020). All these and other advantages make VSV a promising candidate OV for PDAC treatment, and we have shown that VSV is effective against the majority of PDAC cell lines in vitro and in vivo (Moerdyk-Schauwecker et al., 2013; Murphy et al., 2012b). Importantly, several phase I clinical trials using VSV against different malignancies are in progress (ClinicalTrials.gov for trials NCT03647163, NCT02923466, NCT03120624, NCT03865212, and NCT03017820).

VSV exhibits inherent oncotropism based largely on defective or reduced type I IFN responses, as specific genes associated with type I IFN responses are downregulated or functionally inactive (Heiber and Barber, 2011; Moussavi et al., 2010). In addition, IFN signaling can be inhibited by MEK/ERK signaling or by epigenetic silencing of IFN-responsive transcription factors IRF7 or IRF5 (Noser et al., 2007; Zhang et al., 2010). However, some PDACs do not have these defects and resist VSV infection like normal cells, which are sensitive to IFN-α treatment and capable of secreting type I IFNs following VSV infection (Li and Tainsky, 2011).

There has been a demonstration of neurotoxicity in mice infected intranasally or intracranially, demonstrating a need for methods of improvement of VSV oncoselectivity and neurotropic safety without compromising oncolytic ability. There are at least eight approaches demonstrated to address these needs (Felt and Grdzelishvili, 2017c; Hastie et al., 2013b; Hastie and Grdzelishvili, 2012b): (i) mutating the VSV M protein; (ii) VSV-directed IFN-β expression; (iii) attenuation of VSV through disruption of normal gene order; (iv) mutating the VSV G protein; (v) introducing targets for microRNA from normal cells into the VSV genome; (vi) pseudotyping VSV; (vii) experimental adaptation of VSV to cancer cells; and (viii) using semi-replicative VSV. Most of the studies in our laboratory focus on VSV-ΔM51 recombinants containing a deletion of the methionine residue at position 51 of the M protein, VSV-ΔM51. This mutation results in an inability of VSV-M to inhibit nucleus-to-cytoplasm transport of cellular mRNA, including antiviral transcripts, in normal cells with functional antiviral signaling (Petersen et al., 2000; Stojdl et al., 2003).

Our laboratory has characterized numerous human PDAC cells lines and discovered a wide range of susceptibility and permissiveness of different PDAC cell lines to VSV and other tested OVs (Bressy et al., 2019; Cataldi et al., 2015; Felt et al., 2017; Felt et al., 2015; Hastie et al., 2016; Moerdyk-Schauwecker et al., 2013; Murphy et al., 2012b). The range includes “super-permissive” cell lines (such as MIA PaCa-2 and Capan1), “super-resistant” cell lines (such as HPAF-II, Hs766T), and well as many cell lines in between (such as SUIT2 and AsPC-1). Our extensive analysis of a large number of human PDAC cell lines demonstrates that PDAC cell lines show surprising diversity with regard to their ability to produce and respond to type I IFNs, and the evaluation of

IFN sensitivity and IFN-α and IFN-β production within a cell line may be used to predict its responsiveness to oncolytic treatment (Moerdyk-Schauwecker et al., 2013; Murphy et al., 2012b) (Figure 3).

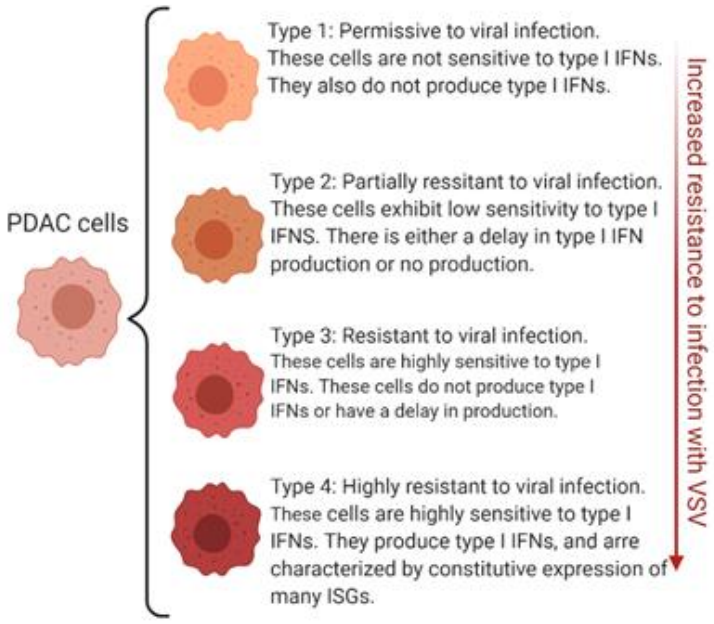

Figure 3. Permissiveness of PDAC to VSV: Four Different Phenotypes. This figure demonstrates the variability across PDAC in regard to permissiveness to infection by VSV. Permissiveness refers to the cells allowance for viral attachment, infection, and replication. This figure was made by Molly Holbrook using Biorender.

Upregulated or residual expression of antiviral genes display four unique phenotypes (Figure 2): (i) no type I IFN production and not responsive to type I IFN, (ii) no type I IFN production but responsive to type I IFN, (iii) type I IFN production and responsive to type I IFN, (iv) super resistant PDACs: type I IFN production, responsive to type I IFN and constitutive expression of many antiviral IFN-stimulated genes (ISGs) (Cataldi et al., 2015; Hastie et al., 2016; Murphy et al., 2012b).

We also conducted a transcriptome analysis to identify biomarkers for resistance of PDAC cell lines to VSV-ΔM51. Of the genes identified, six demonstrate constitutive co-expression in the VSV-resistant cell lines: MX1, EPSTI1, XAF1, GBP1, SAMD9, and SAMD9L (Hastie et al., 2016). Most of these genes are known to have an antiviral effect. Moreover, shRNA-mediated knockdown of MX1 showed a positive effect on VSV-ΔM51 replication in resistant PDAC cells, suggesting that at least some of the identified ISGs contribute to resistance of PDACs to VSV-ΔM51 (Hastie et al., 2016). Finally, we demonstrated that JAK inhibitors effectively break resistance to VSV-ΔM51 while affecting very few non-ISGs, suggesting that the constitutive expression of these genes is likely a causative factor for the phenotype of resistance (Cataldi et al., 2015; Moerdyk-Schauwecker et al., 2013). Further evidence that host antiviral response to VSV-ΔM51 infection is the source of resistance has been shown in infection with WT VSV, as even cell lines resistant to VSV-ΔM51 are permissive to at least some degree to the WT-VSV, which is better able to evade antiviral responses in the host (Moerdyk-Schauwecker et al., 2013; Murphy et al., 2012b).

1.2 Rationale

Pancreatic ductal adenocarcinomas are associated with being highly aggressive, invasive, and resistant to chemotherapy with particularly poor prognosis. Late-stage diagnosis due to limited and ambiguous symptoms and limited treatment options have maintained a high mortality rate, alongside increasing incidence. Even completely resected disease is often recurrent, and it is critical to develop novel, rational approaches to treatment. Vesicular stomatitis virus (VSV) based oncolytic viruses are promising agents against PDAC however not ubiquitously, some PDAC cell lines are resistant to

VSV. This thesis examined two independently conducted screenings of the DiscoveryProbe FDA-Approved Drug Library of 2018. The library, which contains 1,496 FDA-approved drugs, was screened in five different cell lines, including four phenotypically distinct PDAC cell lines with varying degrees of permissiveness to viral infection and one non-malignant cell line to evaluate oncoselectivity of VSV-drug combinations. The complete results of this screening can be found in the supplementary table file. We have identified several promising FDA-approved drugs stimulating VSV replication to varying degrees across the range of PDAC cell lines, which did not exhibit cytotoxicity in non-malignant cells. Interestingly, several commonly used pancreatic cancer chemotherapeutics were seemingly ineffective or even inhibited VSV replication in all five cell lines. There are two levels of beneficence within our study. The first is the potential to identify candidates for combinatorial therapy with oncolytic viruses including VSV through the identification of drugs with positive interactions that stimulate viral infectivity, replication, or oncolysis. The second is the generation of a compendium of interactions between drug treatments patients may be using that could negatively impact OV therapy. This is the first library screening of drug interactions completed with VSV. Our study is critical to the development of rational chemovirotherapy approaches to enhance oncolytic virotherapy efficacy and broaden the spectrum of pancreatic cancers that can be successfully treated.

CHAPTER 2: HYPOTHESIS AND SPECIFIC AIMS

2.1 HYPOTHESES

1. By conducting screenings of multiple PDAC cell lines and the nonmalignant fibroblast cell line, we will be able to identify drugs that stimulate viral replication in PDAC cells (but not in nonmalignant cells) for further evaluation.

2. Fostamatinib increases the oncolytic activity of VSV and other viruses by stimulating viral replication in PDAC cells.

2.2 RESEARCH FOCUS

Evaluating the impact of existing FDA-Approved drugs affecting VSV replication and subsequent oncolytic activity in PDAC to identify drugs that stimulate viral replication as potential combinatorial therapies.

2.3 SPECIFIC AIMS

Aim 1: Identification of FDA Approved drugs stimulating replication of VSV in PDAC

Aim 2: Characterization of the activity of fostamatinib in PDAC cell lines.

CHAPTER 3: LIBRARY SCREENING, ANALYSIS, AND EVALUATION OF FDA-APPROVED DRUGS FOR TREATMENT OF PDAC WITH VSV

3.1 MATERIALS AND METHODS

3.1.1 FDA-Approved Drug Library Screening

The DiscoveryProbe™ Food and Drug Administration (FDA)-approved pharmaceutical drug library of 2018 contains 1496 drugs and is organized into 17 separate 96-well formatted plates (5). In this format, there are columns number 1-12 and rows labeled A-H. The 12th column on the plates were intentionally left empty resulting in the drug tubes holding the substances only being present in columns 1-11. The original plates were stored in a -80°C freezer for preservation. The concentration of the pharmaceutical drugs in the original plates were 10uM in 100% dimethyl sulfoxide (DMSO). Each of the 17 plates were diluted into copy plates of the original by transferring 10uL of drug from the original drug tubes into 90uL of 11.1% DMSO in the wells of a new sterile, untreated 96-well plate. The format of the original plates was maintained in the copy plates for identification of the drugs. For experimentation only, the diluted copies of the original drug plates were again diluted to a concentration of 5 uM by transferring 4uL from the wells of the copy plates into 796uL of Dulbecco's Modified-Eagle Medium (DMEM) (Corning) with 5% fetal bovine serum (FBS) (Gibco) in a sterile, untreated deep well (1000uL capacity) 96-well plate. The full 800uL held in the deep-well 96-well plate was used to treat the 5 cell lines post-infection/aspiration of the virus with 100uL in each of the wells in columns 1-11 on the experimental plates. The five cell lines used (Suit-2, AsPC-1, HPAF-II, Hs766T, and AG01519-Fibroblast 2) were seeded into 96-well plates, infected in columns 1-11 with controls of VSV-ΔM51-GFP

added alone, VSV-ΔM51-GFP and Ruxolitinib (positive control) added, and no drug or VSV-ΔM51-GFP added being separated into wells in column 12. After 1 hour of infection, they had VSV-ΔM51-GFP aspirated and the drugs from the plates of the library added. The VSV-ΔM51-GFP expresses the green fluorescent protein (GFP) and the level of viral replication was detected using a fluorometer. GFP was measured and recorded starting at 1 h p.i. over the course of 96 hours, following infection with VSV-ΔM51-GFP and the addition of drug treatment. The results were evaluated to determine the effects of the drug treatments in all of the cell lines in comparison to the control and virus alone. The effect was calculated as a fold change in GFP for each treatment within the respective cell lines, and all statistical analyses were performed in Excel, and the complete results can be found in the supplementary table.

3.1.2 Ruxolitinib Control

Ruxolitinib was used as a positive control in this screening. Ruxolitinib is a Jak inhibitor which serves to inhibit type I IFN signaling and prevent host cell responses to viral infection. This drug was used to treat wells D-F in column 12 on all five cell plates that had been infected with VSV-**Δ**M51-GFP. Ruxolitinib was diluted to 5uM from a stock solution with a concentration of 2.6mM. This was done by taking 3.76uL of Ruxolitinib and placing it into 1.996 mL of DMEM with 5% FBS and 0.1% DMSO. The wells D-F in column 12 on all five cell plates had 100 mL of the 5 uM Ruxolitinib added to them (matching the concentration of the FDA Library Drugs) after 1-hour post infection.

3.1.3 Fostamatinib as the Candidate Drug

R788 Sodium (also known as Fostamatinib disodium, Syk kinase inhibitor R-935788, Tavalisse, and Tavlesse) was approved by the FDA for medical use in April 2018. It is a tyrosine kinase inhibitor medication often used for the treatment of chronic immune thrombocytopenia (ITP). R788 Sodium blocks the activity of the enzyme spleen tyrosine kinase (Syk) which is responsible for stimulating parts of the immune system. In blocking the activity of Syk, R788 Sodium reduces the immune system's degradation of platelets, thus allowing the platelet count to rise. Its approval was supported with evidence from two clinical trials FIT-1 (NCT02076399) and FIT-2 (NCT02076412).

Syk is associated with a variety of inflammatory cells and has been suggested to be a key player within the complicated mechanisms underlying host immune responses to viral infection. Syk plays a large role in FcγR-mediated signal transduction and inflammatory propagation and may impact many of the interconnected pathways involved in immune responses, and recent data suggests that inhibition of Syk could serve to significantly impair immune activation. The JAK/STAT1 pathway is generally activated by cytokines like type I IFN. Liu et al. demonstrate that a host may establish the initial antiviral immunity by activating the RIG-I/MAVS/Syk pathway that regulates STAT1 phosphorylation in a cytokine-independent manner at the beginning stage of viral infection (Liu et al., 2021).

3.1.4 Viruses and Cell Lines

The cell lines that were used varied in VSV permissibility with Suit-2 and AsPC-1 being more permissible than Hs766T and HPAF-II along with the human fibroblasts AG01519. Each of the cell lines were passed at a maximum of 25 times until new cells were thawed out and a new passage was started. The cells were seeded in volumes of

100uL per well into 96-well plates at 100% confluence. The cells all had their respective medias aspirated and were washed with PBS prior to infection with VSV-ΔM51-GFP at a multiplicity of infection (MOI) of 0.1 for 1 hour at 37 °C in DMEM 0% FBS. For all five plates, an experimental stock solution of 7.8uL of VSV-ΔM51-GFP was placed into 24.49 mL of DMEM. During the period of infection in columns 1-11, 50uL of VSV-ΔM51-GFP from the experimental stock was placed into the wells. After 1 hour, the virus was aspirated and 100uL of the respective drugs were added to all five cell plates. GFP fluorescence measurements were performed over the course of 96 hours using the multi-well plate reader CytoFluor Series 4000 (excitation filter of 485/20 nm, emission 530/25 nm, gain=63; Applied Biosystems). In addition to VSV-ΔM51-GFP, three other viruses were used in assays included in this thesis: VSV-p1-GFP, VSV-rWT-GFP, and SeV-GFP, which will be discussed in detail in the next section.

3.1.5 Multi-Virus Kinetics Confirms Stimulation of Viral Replication

Both Suit-2 and HPAF-II cells were seeded onto one 96-well plate respectively. After cells reached approximately 95% confluency they were infected at MOI 0.1 with either VSV-rWT-GFP, VSV- ΔM51-GFP, VSV-p1-GFP, or SeV in DMEM containing 0% FBS for one hour. After the infection period, viral media was aspirated and cells were washed with PBS to remove unattached viral particles. Cells were then treated with 5uM of either ruxolitinib or fostamatinib, or were mock treated with an equal concentration of DMSO in DMEM containing 5% FBS. GFP was measured at regular intervals over the course of 144 hours, and values were graphed and analyzed using GraphPad Prism.

3.1.6 Western Blot Analysis for Confirmation of Viral Stimulation

Cells were seeded onto two 12-well plates with one drug was assigned to each well. Wells 23 and 24 were designated for the virus control and cells only. AsPC-1 was excluded from the western blot analysis for its inconclusive results. When the seeded cells reached approximately 95% confluency, the virus was added from a stock solution of 5.76uL of virus at MOI 0.1 for Hs766T and HPAF-II and 0.01 for Suit-2 and Fibroblast 2 in 7200uL in DMEM with 0% FBS (per cell line) in the volume of 250uL/well. After an incubation period of 1 hour of infection at 37 °C, the media was aspirated and the drugs were added to the proper wells at 2.5 M in DMEM with 5% FBS and 0.1% DMSO. At 30 hours post infection for Suit-2 and Fibroblast 2 and 48 hours post infections for Hs766T and HPAF-II, the media was aspirated from each plate, GFP fluorescence was measured, and the cell lysates were collected after being washed three times with PBS to ensure the removal of unattached virus particles. Total protein was isolated using a lysis buffer containing 1M Tris-HCl (pH 6.8), 10% glycerol, 2% SDS, 5% beta-mercaptoethanol and 0.02% (w/v) bromophenol blue. Total protein was separated by electrophoresis on SDS-PAGE gels and electro-blotted to polyvinylidene difluoride (PVDF) membranes. Membranes were blocked using 5% non-fat powdered milk in TBS-T (0.5 M NaCl, 20 mM Tris (pH 7.5), 0.1% Tween-20). Membranes were incubated in TBS-T with 5% BSA or milk with 0.02% sodium azide. VSV was used to probe and Coomassie was used for loading control in the Coomassie stain.

3.1.7 Viral Kinetics and Particle Production

Suit-2 and HPAF-II cells were seeded onto four 6-well plates respectively. After cells reached approximately 95% confluency, media was aspirated and cells were washed with PBS. Cells were then infected with VSV- **Δ**M51-GFP at MOI 0.1 in DMEM

containing 0%FBS for one hour before virus was aspirated and cells were washed three times with PBS to remove unattached viral particle. After infection, cells were treated with either mock, 5uM ruxolitinib or 5uM fostamatinib in DMEM containing 5% FBS. GFP was scanned over the course of the treatment period and at each pre-determined timepoint media was collected. Collected media was used to titer virus on BHK-21 cells as a measure of de novo particle production from infected cells. For BHK-21 titers, six 96-well plates were seeded with BHK-21 cells and infected with serial dilutions of collected media samples, starting with a dilution of 1E-4 with 5-fold dilutions proceeding to 1E-11 in DMEM containing 0% FBS. After an infection period of one hour, viral media was aspirated and replaced with DMEM containing 5%FBS. After 18 hours, fluorescent foci were counted and used to calculate viral titer in PFU/mL which were then graphed alongside GFP kinetics with GraphPad Prism.

3.1.8 Stimulated Oncolytic Activity by Plaque Assay

Three 12-well plates were seeded for with either Suit-2 or HPAF-II. Cells were infected with 3-fold serial dilutions of VSV-ΔM51-GFP for one hour. Suit-2 cells were infected with serial dilutions of viral media starting at 1.0E-4 and ending 1.7E-9 with the final well mock treated, while HPAF-II cells were infected with serial dilutions starting at 1.0E-2 and ending at 1.7E-7. After infection, viral media was aspirated and cells were washed with PBS before media containing drug treatment with 5%FBS and 2% bactoagar was replaced. Cells were treated with mock, 5uM ruxolitinib, or 5uM fostamatinib. After the media solidified, cells were incubated at 37C for 72 hours before being fixed with formalin for two hours. After fixation, the agar overlay was removed and cells were

stained with crystal violet for 15 minutes. After staining was completed, cells were washed three times with diH2O.

3.1.9 Viral Kinetics Comparing Timing of Treatment Relative to Infection

Suit-2 and HPAF-II cells were each seeded onto three different 96-well plates. Cells were pre-treated with drug 4 hours after seeding to allow time for cellular attachment to the well surface and infected 24 hours later with several dilutions of fostamatinib starting at 5000nM and ending at 5nM in DMEM containing 0% FBS. Prior to infection, media was aspirated and cells were washed with PBS. Cells were infected for one hour prior to the addition of post-treatment to the appropriate samples. GFP was measured immediately following infection over the course of 120 hours and graphed with GraphPad Prism.

3.1.10 Western Blot for Drug Induced Antiviral Signaling

Suit-2 and HPAF-II cells were seeded onto one 24-well plate each. After reaching approximately 95% confluency, cells were pre-treated with an inducing agent of antiviral signaling, either 10uM Poly(I:C), 1ug/mL LPS, 5000u/mL IFN-α, or mock treatment in DMEM containing 5% FBS for 2 hours. After pre-treatment, media was aspirated and drug treatment of either 5uM Ruxolitinib or Fostamatinib, or mock was administered for an additional 2 hours in DMEM containing 5% FBS, for 4 hours of treatment total. Once the treatment period concluded, total protein was isolated using a lysis buffer containing 1M Tris-HCl (pH 6.8), 10% glycerol, 2% SDS, 5% beta-mercaptoethanol and 0.02% (w/v) bromophenol blue. Total protein was separated by electrophoresis on SDS-PAGE gels and electro-blotted to polyvinylidene difluoride (PVDF) membranes. Membranes were blocked using 5% bovine serum albumin in TBS-T (0.5 M NaCl, 20 mM Tris (pH

7.5), 0.1% Tween-20). Membranes were then incubated in TBS-T with 5% BSA with primary antibody for each protein probed.

3.1.11 Western Blot for Cellular Response to Viral Infection

Cells were seeded onto four 6-well plates with either cell line. Cells were infected with VSV- **Δ**M51-GFP at MOI 0.1 in DMEM containing 0%FBS for one hour before virus was aspirated, and then treated with either mock, 5uM Ruxolitinib or Fostamatinib in DMEM containing 5% FBS. Total protein was isolated using a lysis buffer containing 1M Tris-HCl (pH 6.8), 10% glycerol, 2% SDS, 5% beta-mercaptoethanol and 0.02% (w/v) bromophenol blue. Total protein was then separated by electrophoresis on SDS-PAGE gels and electro-blotted to polyvinylidene difluoride (PVDF) membranes. Membranes were blocked using 5% bovine serum albumin in TBS-T (0.5 M NaCl, 20 mM Tris (pH 7.5), 0.1% Tween-20). Membranes were incubated in TBS-T with 5% BSA with primary antibody for each protein probed.

3.1.12 Interferon Production in Response to VSV Infection

Both Suit-2 and HPAF-II cells were seeded onto a single 96-well plate, with rows A-D seeded with Suit-2 and rows E-H seeded with HPAF-II. The first two columns were left empty for the appropriate standards for each ELISA kit, and the remaining 10 columns were used to collect samples. For each cell line, the first row was mock treated, the second was infected with VSV only, the third and fourth rows were infected with VSV and treated with ruxolitinib and fostamatinib respectively. Suit-2 cells were infected at MOI 0.01 and HPAF-II cells were infected at MOI 0.1. After cells reached 100% confluency, cellular media was aspirated and cells were washed with PBS. After washing, cells were treated with mock media containing DMSO in the same

concentration as drug treated cells, 5000nM ruxolitinib, or 5000nM fostamatinib in DMEM containing 5% FBS. Samples were prepared in triplicate for each timepoint of collection, with columns 3-5 collected 8 h after treatment, columns 6-8 collected 24 h after treatment, and columns 9-11 collected 48 h after treatment. Column twelve was collected 0 h after treatment as a positive control for each treatment. At each timepoint, media was collected and each sample was diluted with the addition of 350uL of media, to make sufficient volume for each ELISA kit. IFN-α was evaluated using the Verikne™ Human IFN-α Multi-Subtype ELISA Kit by pbl assay science, product # 41105 according to lot-specific manufacturer protocol. IFN-β was evaluated using the Verikne™ Human IFN Beta ELISA Kit by pbl assay science, catalog # 41410 according to lot-specific manufacturer protocol. IFN-λ (IL-28A) was evaluated using Human IL-28A ELISA Kit by Invitrogen, catalog # EHIL28A according to lot-specific manufacturer protocol.

3.2 RESULTS

3.2.1 FDA-Approved Drug Library Screening to Identify Drugs Affecting VSV Replication in PDAC Cell Lines

The processes of discovery of novel drugs, development, and seeking approval for use are a significant hurdle for developing effective treatment approaches to any disease, especially in the case of PDAC treatments where there is great need. We sought to evaluate how already-approved drugs impact efficacy of OV treatment, which allows us to bypass several of these processes and informs both of potential negative reactions to avoid and positive reactions that may benefit treatment. The library screening was conducted in two independent and simultaneous screening with all five cell lines. GFP-driven viral kinetics were measured over the course of 96 hours as an indirect measure of

viral replication. We have previously demonstrated that GFP is strongly correlated with viral production within the cells. From this data, Supplementary Table 1. was formatted highlighting the effects of the drug treatments in all the cell lines as compared to the control drug treatment with ruxolitinib. The effect was as a fold change in GFP over 48 h p.i. for each drug within all of cell lines. Of the 1,496 drugs in the library, 22 drugs of interest, including ruxolitinib, were evaluated further by western blot analysis probing for viral proteins after infection, and these data combined lead to our selection of fostamatinib as our current candidate drug, and the outline of this experimental setup can be seen in Figure 4.

3.2.2 Confirmation of the Effect by Fostamatinib on Viral Stimulation in PDAC

The initial results from the library screening demonstrated a positive effect in stimulating viral replication in PDAC cells, even those typically resistant to viral infection with treatment at a single concentration of 5uM. We infected both Suit-2 and HPAF-II cells with four different replication-competent viruses with different degrees of infectivity. Those viruses included VSV-ΔM51-GFP as in the previous experiments, VSV-rWT-GFP, VSV-p1-GFP, and SeV. The rWT virus is wild-type VSV with the GFP reporter gene inserted in the viral genome at the fourth intergenic sequence. The p1 VSV is also wild-type VSV, however the GFP is inserted at the first intergenic sequence, resulting in much greater GFP production. SeV or Sendai virus is a single-stranded negative-sense RNA virus that replicates in the cytoplasm, as is VSV. As demonstrated in Figure 5., Suit-2 cells infected with VSV-ΔM51-GFP, there was no significant difference between ruxolitinib and fostamatinib treated cells, however both demonstrated greater viral replication than mock treated cells. For the other VSVs, there was no difference in

GFP regardless of treatment. In SeV infected cells, fostamatinib treated cells demonstrated the greatest amount of viral replication. In HPAF-II there was no difference between fostamatinib or ruxolitinib treated cells, but mock treated cells did not demonstrate any degree of viral replication.

Both the previous results indicated stimulated viral replication by GFP, and we next wanted to confirm that increased GFP is also associated with increased viral protein abundance as a secondary evaluation. In Figure 6. western blot analysis confirms stimulated viral replication of VSV in the cell lines by several of the selected drugs in Suit-2. The western blot analysis shows increased abundance of viral protein in ruxolitinib and R788 Sodium (Fostamatinib) treated cells in all PDACs, and they are the only samples that show increased protein in HPAF-II. In Hs766T, Idarubicin and Dinaciclib also show an increased amount of viral protein present after infection relative to VSV alone. It is also important to note that ruxolitinib and dinaciclib also show increased viral protein in AG01519, the nonmalignant fibroblast. AsPC-1 was excluded from the analysis because results were inconclusive.

Our results indicated stimulated viral replication on the levels of both GFP and viral protein expression by two different methods of evaluation, and we next wanted to evaluate if particle production was similarly increased. Cells were infected prior to being treated with either mock, 5uM ruxolitinib or 5uM fostamatinib. GFP was scanned over the course of 48 h and at each pre-determined timepoint media was collected and used to titer virus on BHK-21 cells as a measure of *de novo* particle production from infected cells. Suit-2 cells were infected with VSV- ΔM51-GFP at MOI 0.01. There was no difference between titers of ruxolitinib and fostamatinib treated cells, which spiked at 36

h p.i. GFP values for ruxolitinib treated cells were significantly higher than mock treated cells by 24 h p.i. and remined significantly higher, and fostamatinib treated cells showed increased GFP by 36 h p.i. remained so through 48 h p.i. HPAF-II cells were infected with VSV- ΔM51-GFP at MOI 0.1. GFP values for both ruxolitinib and fostamatinib treated cells were significantly higher at 36 h p.i. and remained so at 48 h p.i.

3.2.3 Fostamatinib Stimulates Oncolytic Activity of VSV

From our previous results, we determined that treatment of PDACs with fostamatinib stimulates viral replication, as demonstrated by increased expression of GFP in cells, viral protein abundance, and viral particle production over the course of infection. The initial benefit served by oncolytic virotherapy is the direct lysis of cancer cells, as we discussed previously. In Figure 8. increased oncolytic activity is also demonstrated by cellular clearance as a direct result of fostamatinib stimulated viral replication and particle production. The abundance and size of plaques are greater in both Suit-2 and HPAF-II cell lines following infection and treatment, and the increased amount of cell lysis after infection is increased, especially in HPAF-II which is very resistant to virus. In mock treated Suit-2, plaques are visible only down to dilutions as low as 3.7E-6, while there are no detectable plaques in mock treated HPAF-II cells, even at the lowest dilution of 1.0E-2. However, in ruxolitinib and fostamatinib treated Suit-2, plaques remain detectable at 4.6E-8 and in HPAF-II cells at 1.4E-5.

3.2.4 Timing of Treatment is Important for Effective Stimulation of VSV

In previous experiments, drug treatment was administered post-infection when infectious media was removed, and we wanted to evaluate whether the effect was reversible by administering treatment prior to infection only, or if treatment before and

after infection would show a greater degree of viral stimulation. We infected both Suit-2 and HPAF-II cells with VSV-ΔM51-GFP at MOI 0.01 and 0.1 respectively. We then treated cells with multiple dilutions of fostamatinib starting at 5000nM and ending at 5nM, or with mock containing equivalent concentration of DMSO, demonstrated in Figure 9. There was not much difference in Suit-2 cells treated post-infection only or cells treated both pre- and post-infection, which were both slightly higher than cells treated pre-infection alone. In HPAF-II cells pre-infection treatment alone was insufficient to break cellular resistance to VSV infection and there was no discernable difference between mock and infected cells at any concentration of drug treatment. However, in post-infection treated cells there was an observable increase in the GFP of cells treated with 5000nM fostamatinib, and in cells treated both pre- and post-infection there was a slight increase in the degree of viral stimulation relative to those treated post-infection only.

3.2.5 Fostamatinib Demonstrates a Novel Mechanism of Activity for Viral Stimulation

After multiple experiments confirming the results of the library screening, we were confident that fostamatinib stimulated viral replication in PDAC cells, but were uncertain about the mechanism of this activity. We first wanted to evaluate whether fostamatinib and ruxolitinib would demonstrate a similar response to drug-induced antiviral signaling without infection. We stimulated an immune state within the cells by treating both Suit-2 and HPAF-II with either LPS, Poly(I:C), IFN-α, or mock for 2 hours. We then removed the stimulatory drugs and replaced media with either ruxolitinib, fostamatinib, or mock drug treatment for an additional two hours prior to collecting total

protein from cell lysates, which can be seen in Figure 10. Suit-2 treated with exogenous IFN-α showed strong STAT-1 phosphorylation in both mock and fostamatinib treated cells, while only ruxolitinib treatment prevented STAT1 phosphorylation. Similarly, HPAF-II cells 2 treated with exogenous IFN-α showed strong STAT-1 and STAT-2 phosphorylation in both mock and fostamatinib treated cells, while ruxolitinib treatment prevented phosphorylation.

The same response was not demonstrated when the induction of antiviral signaling occurred as a result of direct viral infection, rather than by or other drug induction. The pattern of antiviral signaling proteins stimulated with viral infection demonstrates that fostamatinib may be able to down-regulate type I IFN responses by a noncanonical pathway through multiple additive mechanisms of action. We infected both Suit-2 and HPAF-II cells with VSV-ΔM51-GFP and treated the cells with either ruxolitinib or fostamatinib. We then collected viral media and protein lysates over 48 hours and probed for viral protein, common ISGs, and antiviral signaling, demonstrated in Figure 11. We once again saw that viral protein was much more abundant in cells treated with either ruxolitinib or fostamatinib, confirming previous results. We also saw that ISGs like MX1 and OAS2 were not significantly impacted by fostamatinib treatment HPAF-II, although OAS2 expression was similar in Suit-2 cells between ruxolitinib and fostamatinib treated cells, which was lower than mock treated cells, as can be seen in Figure 10.

Viral proteins were detectable in infected cells by 24 h p.i. with no observable difference between treatments. Suit-2 samples collected at 36 h p.i. and 48 h p.i. showed more abundant viral protein in both Ruxolitinib and fostamatinib treated cells. pSTAT1

and pSTAT3 were stimulated in mock treated cells at 24, 36, and 48 h p.i. and were downregulated in ruxolitinib and fostamatinib treated cells. pSyk was detectable in all samples except fostamatinib treated cells collected at 36 and 48 h p.i. pMAPK was stimulated in mock treated cells at 36 and 48 h p.i, with slight downregulation in ruxolitinib treated cells, with greater downregulation in fostamatinib treated cells. OAS2 was stimulated in infected mock treated cells at 24, 36, and 48 h p.i. and was downregulated in the infected cells treated with ruxolitinib or fostamatinib at the same timepoints. MX1 was stimulated in infected mock treated cells at 24, 36, and 48 h p.i. and was downregulated in the infected cells treated with ruxolitinib or fostamatinib at the same timepoints.

HPAF-II samples collected at 36 h p.i. and 48 h p.i. showed more abundant viral protein in both ruxolitinib and fostamatinib treated cells in comparison to mock treated infected cells. pSTAT1 phosphorylated at Y701 was stimulated in mock treated and fostamatinib treated cells at 36 and 48 h p.i. and was downregulated in ruxolitinib treated cells. At phosphorylation position S727, pSTAT1 was detected for all treatments, but was most abundant in mock treated cells. pSTAT2 was stimulated in samples collected at 36 and 48 h p.i. with greater amounts in ruxolitinib treated cells at 48 h p.i. and fostamatinib treated cells were less abundant than both ruxolitinib and mock treated cells. pSTAT3 was stimulated only in mock treated cells. pSyk was detectable in all mock and ruxolitinib treated cells. pMAPK was stimulated in ruxolitinib treated cells at 36 and 48 h p.i, with slightly less in ruxolitinib treated cells, with even less in fostamatinib treated cells. OAS2 and MX1 were stimulated in mock and fostamatinib treated cells at 36 and 48 h p.i. and were downregulated in ruxolitinib and fostamatinib treated cells.

Finally, we wanted to directly observe whether there were differences in cellular cytokine signaling by testing for production of interferons α, β, and λ. We collected cellularly secreted cytokines after infection over a period of 48 hours, which can be seen in Figure 12. In Suit-2 cells, IFN-α was found to be induced in mock treated cells at 48 h p.i., but was suppressed by both ruxolitinib and fostamatinib treatment, and none was detected in HPAF-II. IFN-β was detected in mock treated Suit-2 cells at 24 and 48 h p.i., with significantly lower expression in cells treated with ruxolitinib and fostamatinib. Interestingly, in HPAF-II cells, IFN-β expression was only detected in cells treated with ruxolitinib, and to a lesser extent, fostamatinib at 48 h p.i. It would appear that the effect observed is dependent on the nature of the cell line. As stated previously, Suit-2 is a cell line that exhibits some permissiveness to VSV infection, but is capable of producing interferons in response to infection, as shown in the mock treated samples. However, treatment with ruxolitinib inhibits Jak protein, which prevent STAT phosphorylation and the subsequent production of cytokines within the cell, and therefore the stimulation of any ISGs. In HPAF-II cells, VSV alone is not capable of infection and treatment with ruxolitinib or fostamatinib is necessary to allow any viral replication to take place, at which point antiviral signaling is actually stimulated and we begin to see production of these cytokines.

3.3 Figures and Tables

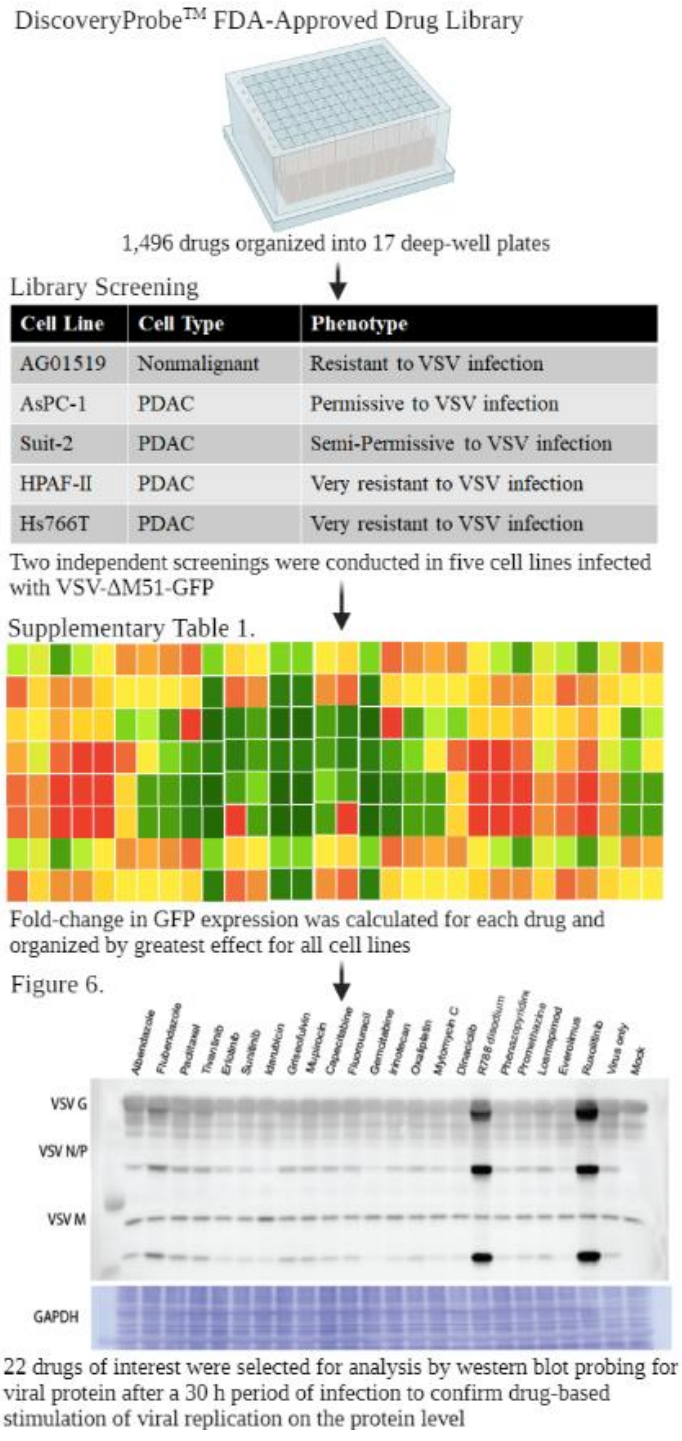

Figure 4: Complete Screening of FDA-Approved Drugs with VSV
This figure illustrates the experimental design for the complete library screening of FDA-Approved drugs in 5 cell lines, resulting in the generation of Supplementary Table 1. And Figure 6. This figure was made by Molly Holbrook using Biorender.

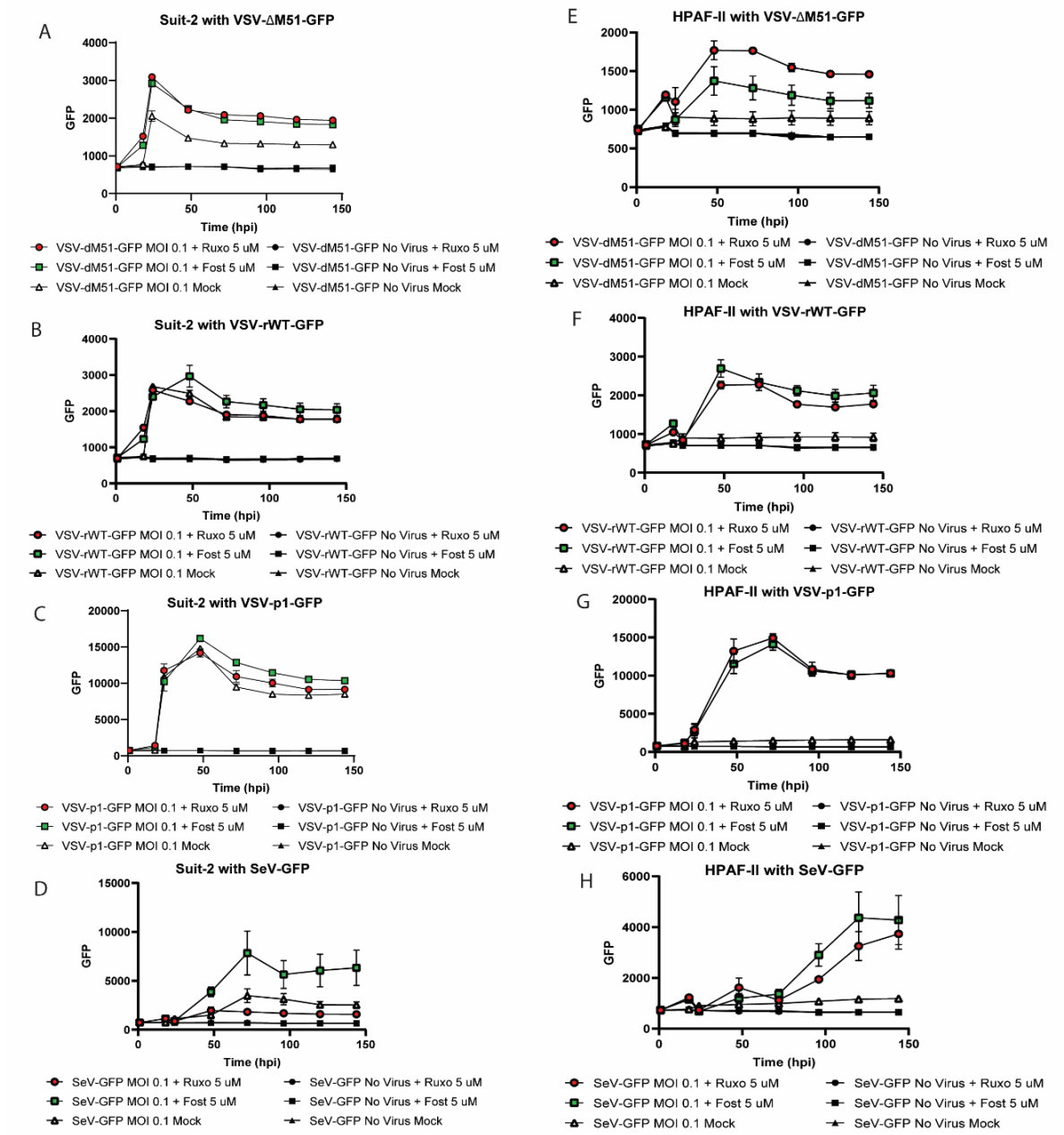

Figure 5. Multi-Virus Kinetics Confirms Stimulation of Viral Replication
Cells were infected with at MOI 0.1 with DMEM containing 0% FBS for one hour. After infection viral media was aspirated and cells were treated with 5uM of either Ruxolitinib or Fostamatinib, or were mock treated with an equal concentration of DMSO in DMEM containing 5% FBS. GFP was measured at regular intervals over the course of 144 hours, and values were graphed with GraphPad Prism. (A) Suit-2 cells were infected with VSV-**Δ**M51-GFP. (B) Suit-2 cells were infected with VSV-rWT-GFP. (C) Suit-2 cells were infected with VSV-p1-GFP. (D) Suit-2 cells were infected with SeV-GFP. (E) HPAF-II cells were infected with VSV- **Δ**M51-GFP. (F) HPAF-II cells were infected with VSV-rWT-GFP. (G) HPAF-II cells were infected with VSV-p1-GFP. (H) HPAF-II cells were infected with SeV-GFP.

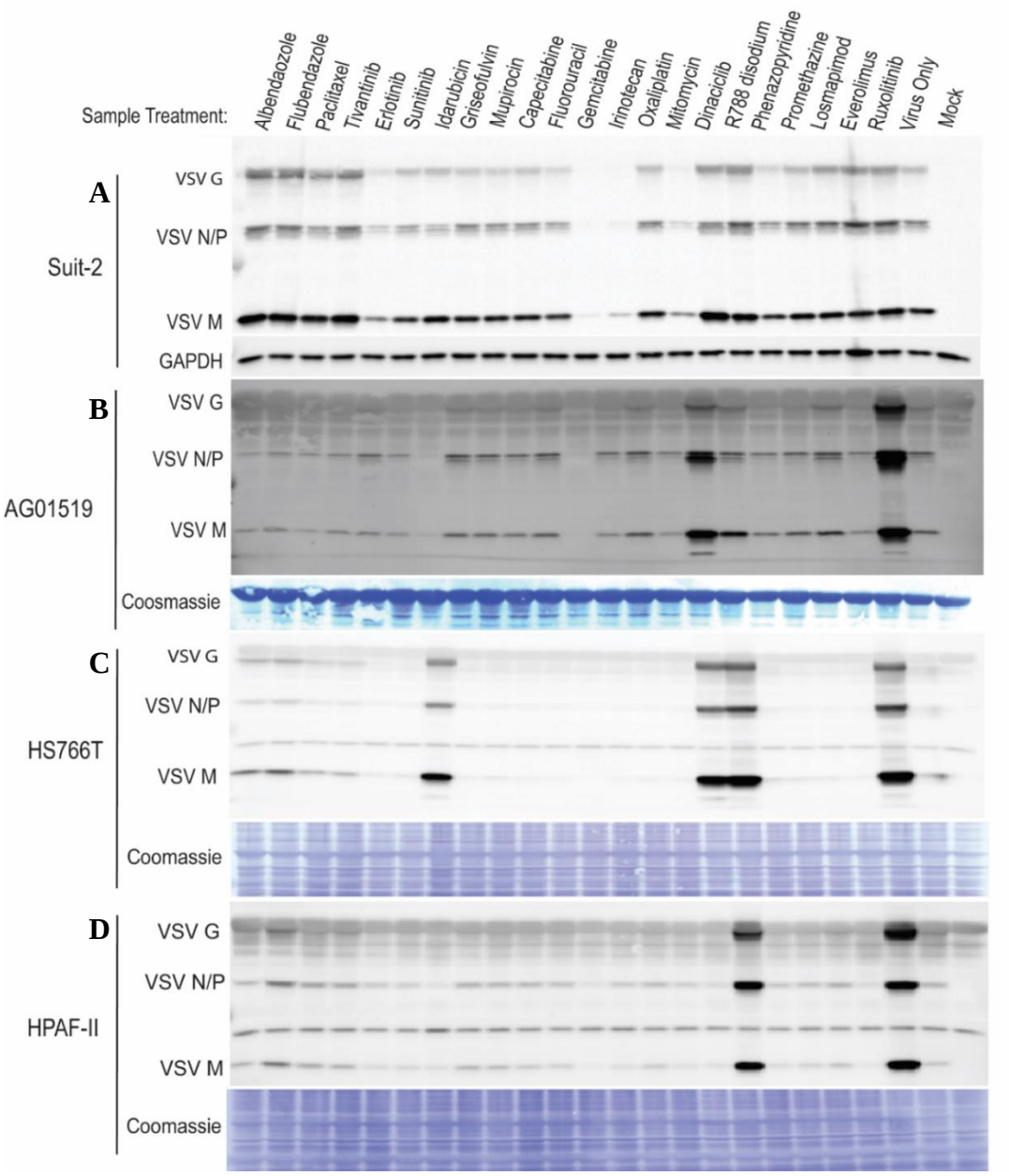

Figure 6. Western Blot Analysis for Confirmation of Viral Stimulation
(A) Suit-2 cells were infected at MOI 0.01 for one hour prior to drug treatment at 2.5uM for each respective drug, and total protein was collected at 30 h p.i. (B) AG01519 cells were infected at MOI 0.01 for one hour prior to drug treatment at 2.5uM for each respective drug, and total protein was collected at 30 h p.i. (C) Hs766T cells were infected at MOI 0.1 for one hour prior to drug treatment at 2.5uM for each respective drug, and total protein was collected at 48 h p.i. (D) HPAF-II cells were infected at MOI 0.1 for one hour prior to drug treatment at 2.5uM for each respective drug, and total protein was collected at 48 h p.i. Membranes were probed for viral protein, and then either (A) probed for GAPDH or (B-D) stained with Coomassie as a loading control.

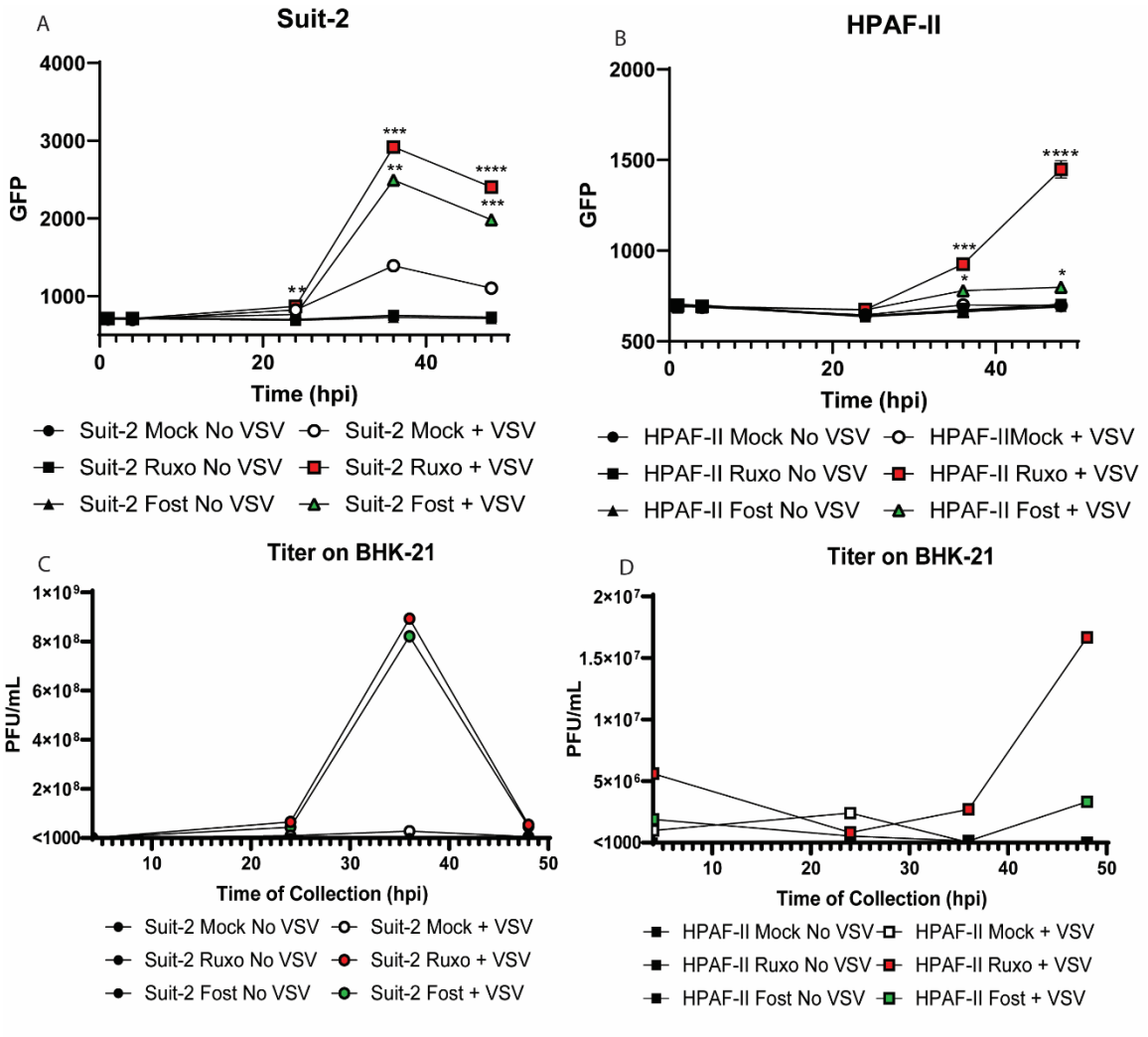

Figure 7. Viral Kinetics of Stimulated Particle Production
Cells were infected prior to being treated with either mock, 5uM ruxolitinib or 5uM fostamatinib in DMEM containing 5% FBS. GFP was scanned over the course of 48 h and at each pre-determined timepoint media was collected. Collected media was used to titer virus on BHK-21 cells as a measure of de novo particle production from infected cells. (A, B) Suit-2 cells were infected with VSV- ΔM51-GFP at MOI 0.01. (A) There was no difference between titers of ruxolitinib and fostamatinib treated cells, which spiked at 36 h p.i. (B) GFP values for ruxolitinib treated cells were significantly higher than mock treated cells by 24 h p.i., p-value 0.005, and remined significantly higher for 36 h p.i. and 48 h p.i., p-values 0.0009 and 0.00009 respectively and for fostamatinib treated cells by 36 h p.i., p-value 0.004, and remained so through 48 h p.i., p-value 0.0007. (C, D) HPAF-II cells were infected with VSV- ΔM51-GFP at MOI 0.1. (D) GFP values for both ruxolitinib and fostamatinib treated cells were significantly higher at 36 h p.i., p-values 0.004 and 0.04 respectively, and remained so at 48 h p.i., p-values 0.0008 and 0.04 respectively.

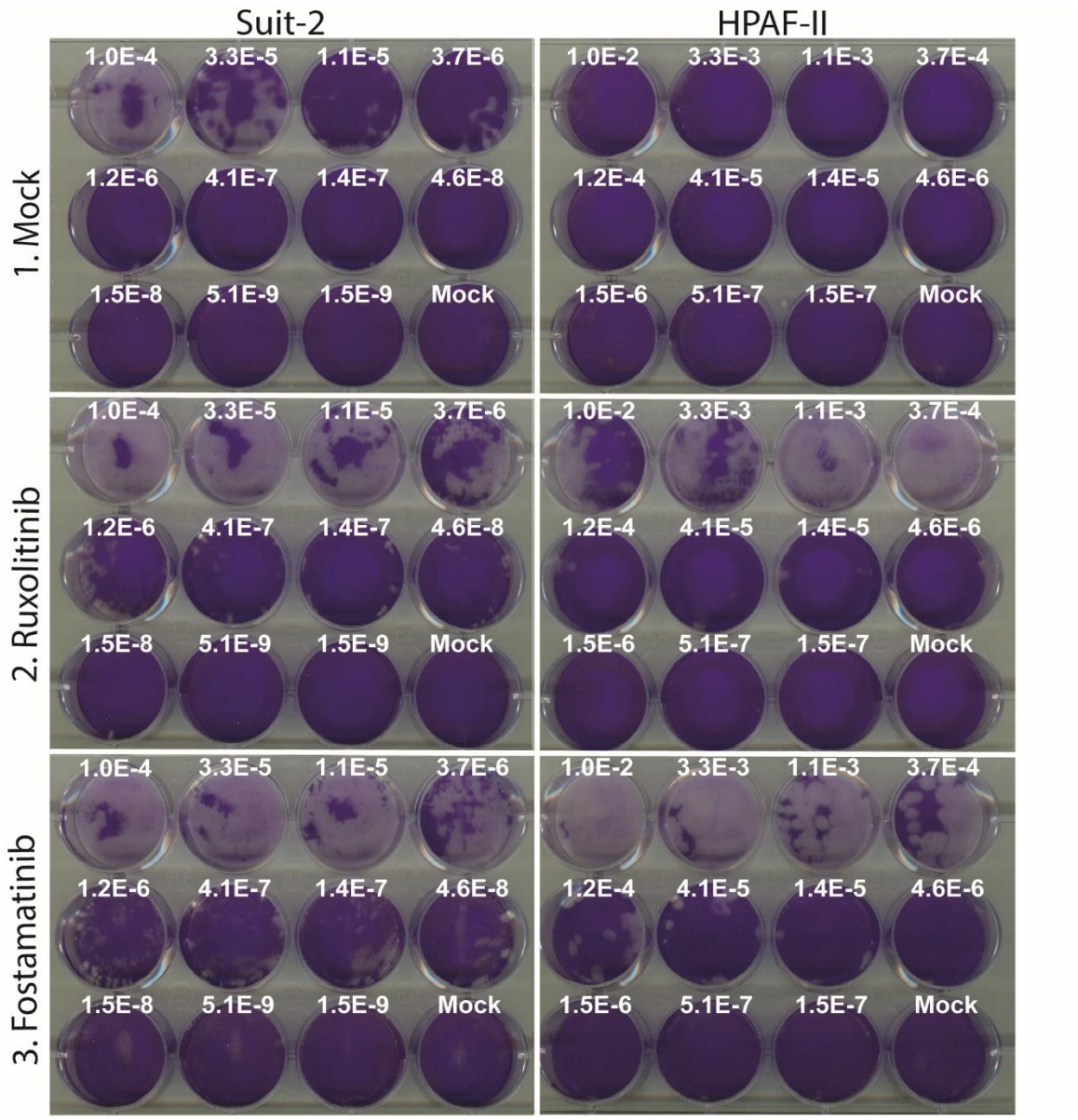

Figure 8. Stimulated Oncolytic Activity by Plaque Assay

Three 12-well plates were seeded with either Suit-2 or HPAF-II cells. Cells were infected with 3-fold serial dilutions of VSV-ΔM51-GFP. Suit-2 cells were infected with serial dilutions starting at 1.0e-4 and ending 1.7e-9 with the final well as uninfected mock, while HPAF-II cells were infected with serial dilutions starting at 1.0e-2 and ending at 1.7e-7 with the final well as uninfected mock. For each cell line, plate 1 was mock treated, plate 2 was treated with 5000nM ruxolitinib, and plate 3 was treated with 5000nM fostamatinib.

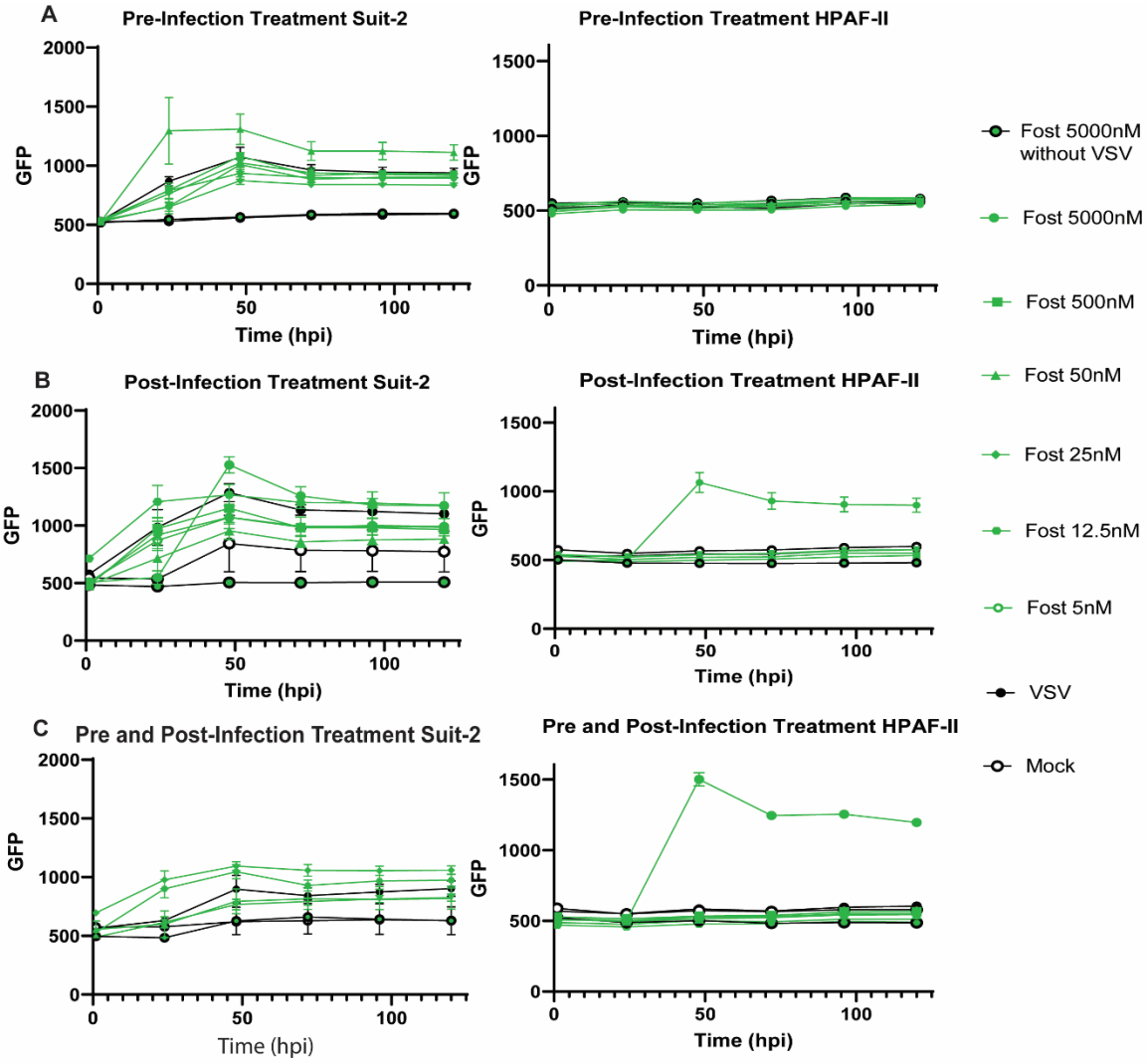

Figure 9. Viral Kinetics Comparing Timing of Treatment Relative to Infection
Cells were seeded onto three 96-well plates per cell line. Suit-2 cells were infected at MOI 0.01and HPAF-II cells were infected at MOI 0.1 with VSV-ΔM51-GFP. Cells were treated with several dilutions of fostamatinib starting at 5000nM and ending at 5nM. (A) Cell were treated pre-infection 4 hours after seeding and infected 24 hours later. Cells were infected for one hour prior to media replacement without drug treatment. (B) Cell were seeded and infected 28 hours later for one hour prior to media replacement with post-infection treatment. (C) Cells were treated pre-infection 4 hours after seeding and infected 24 hours later. Cells were infected for one hour prior to media replacement with post-infection treatment. GFP was measured over the course of 120 h p.i. Viral kinetics were graphed using GraphPad Prism software.

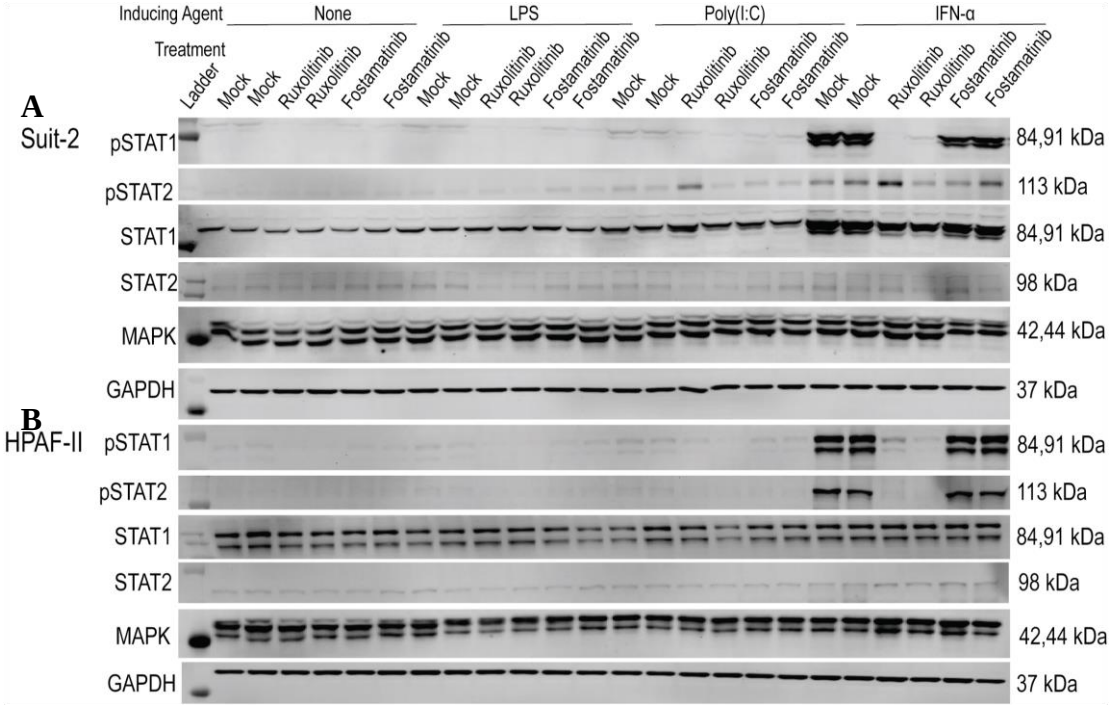

Figure 10. Western Blot for Drug Induced Antiviral Signaling
One 24-well plate was seeded for each cell line. Cells were pre-treated with either 5uM Ruxolitinib or Fostamatinib, or mock for 2 hours. After pre-treatment, media was aspirated and drug treatment with an inducing agent of antiviral signaling, either 10uM Poly(I:C), 1ug/mL LPS, 5000u/mL IFN-α, or mock treatment in DMEM containing 5% FBS for an additional 2 hours in DMEM containing 5% FBS, for 4 hours of treatment total. Once the treatment period concluded, total protein was isolated. (A) pSTAT1 was stimulated in IFN-α stimulated cells but down-regulated by treatment with ruxolitinib. (B) pSTAT1 and pSTAT2 were stimulated in IFN-α stimulated cells but down-regulated by treatment with ruxolitinib.

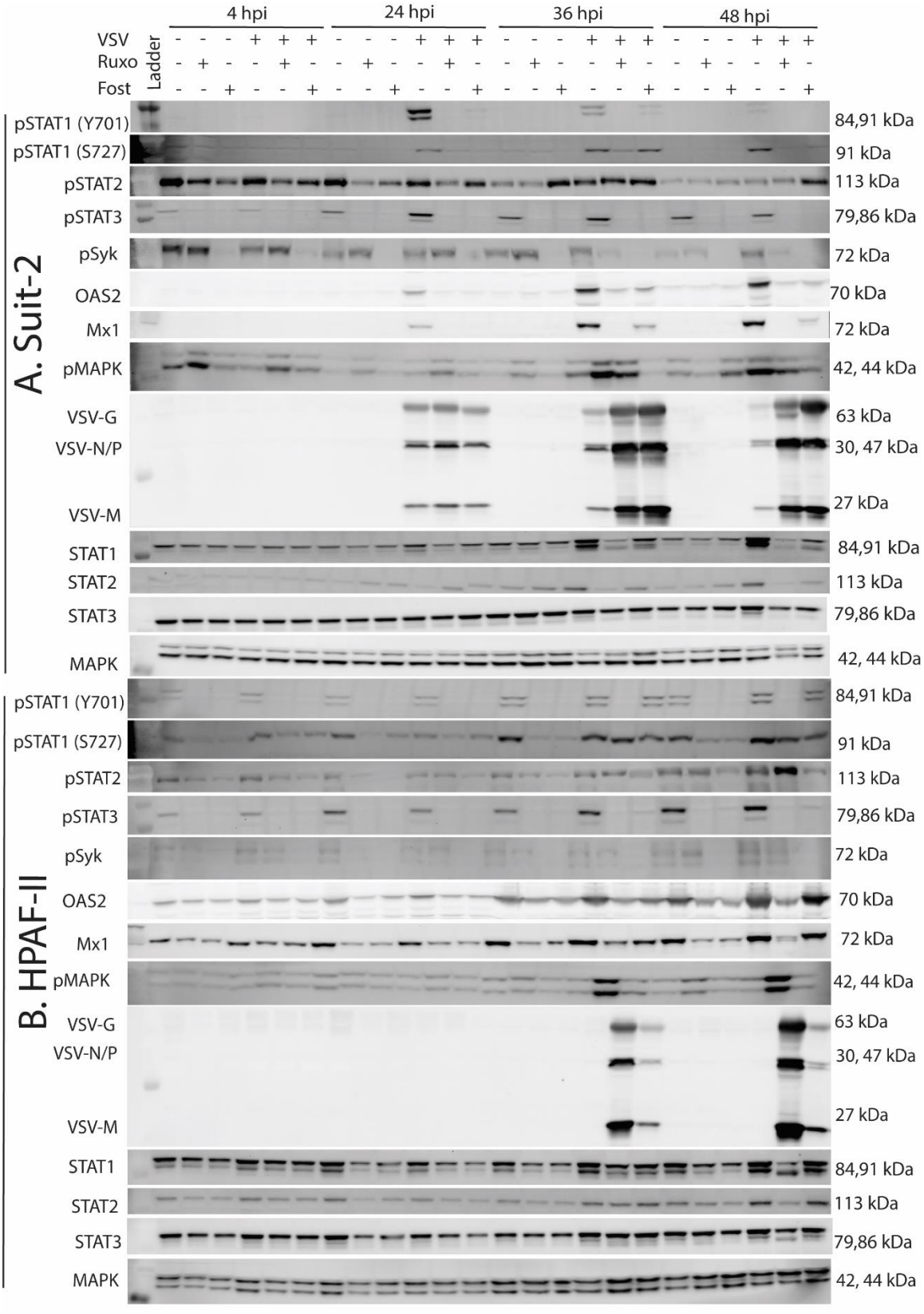

Figure 11. Western Blot for Cellular Response to Viral Infection

Cells were infected with VSV- **Δ**M51-GFP at MOI 0.1 in DMEM containing 0% FBS for one hour before virus was aspirated, and then treated with either mock, 5uM ruxolitinib or 5uM fostamatinib in DMEM containing 5% FBS. Total protein was isolated at each of the pre-determined timepoints and separated by SDS-PAGE gel electrophoresis. (A) Suit-2 cells were infected at MOI 0.01. Membranes were probed for viral protein and antiviral signaling proteins stimulated in response to viral infection. (B) HPAF-II cells were infected at MOI 0.1. Viral proteins were detectable in infected cells by 36 h p.i. Membranes were probed for viral protein and antiviral signaling proteins stimulated in response to viral infection.

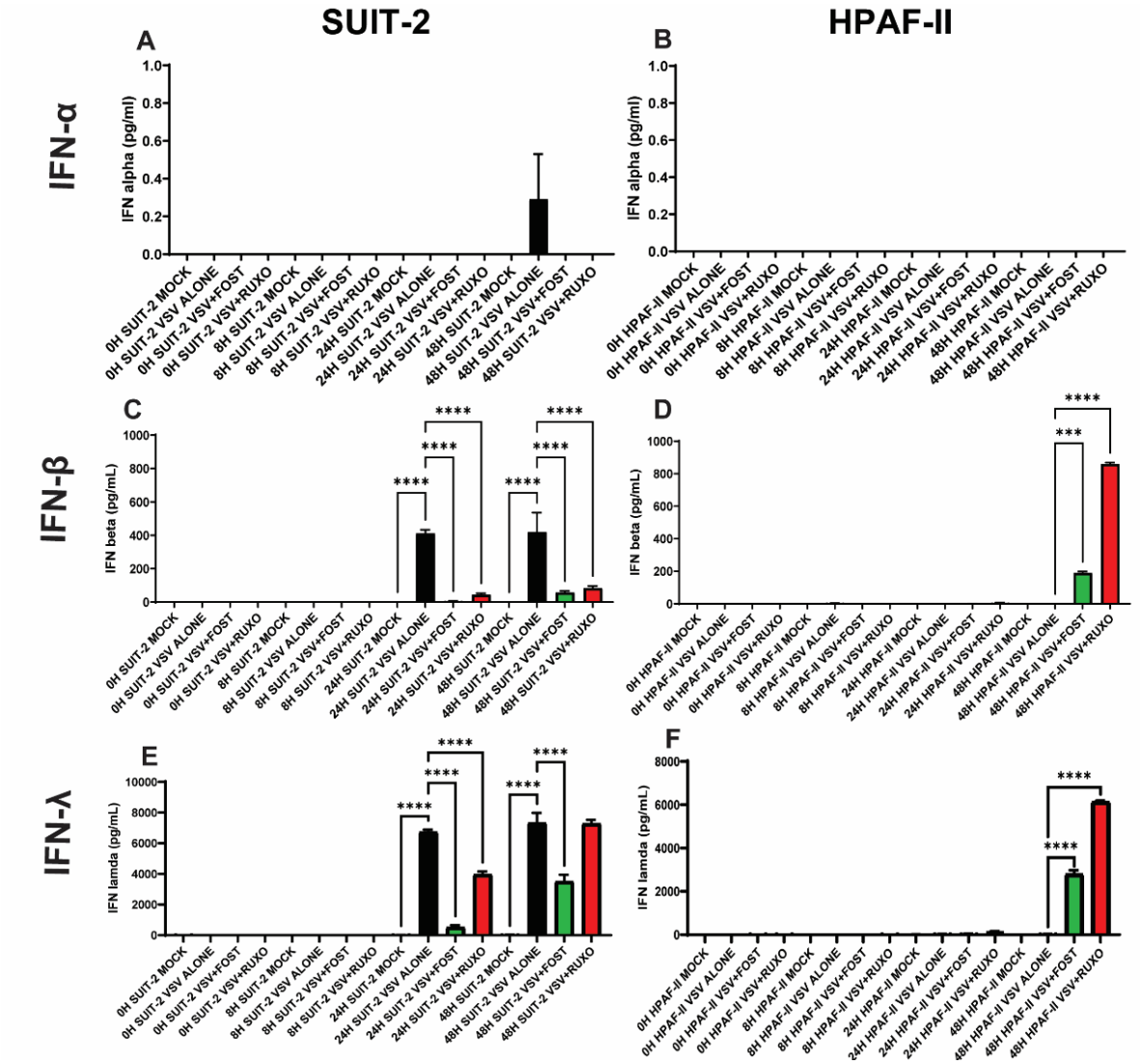

Figure 12. Interferon Production in Response to VSV Infection
(A) Cellular secretions from Suit-2 were collected over the course of 48 h and cytokine production was measured by Verikine™ IFN-Alpha ELISA kit, which resulted in undetectable or nonsignificant amounts of IFN-α at any timepoints. (B) Cellular secretions were collected over the course of 48 h and cytokine production was measured by Verikine™ IFN-Alpha ELISA kit, which resulted in undetectable or nonsignificant amounts of IFN-α at any timepoints. (C) Cellular secretions from Suit-2 were collected over the course of 48 h and cytokine production was measured by Verikine™ IFN-Beta ELISA kit, which resulted in significantly increased IFN-β in cells infected with VSV alone compared to mock at both 24 and 48 h p.i., p-values <0.0001. There was no statistical difference between the amount of IFN-β between mock treated cells in comparison to either fostamatinib or ruxolitinib treated cells. There was a significant difference in the amount of IFN-β of VSV only cells in comparison to both fostamatinib and ruxolitinib treated cells at both 24 and 48 h p.i., all of which were p-value <0.0001. Treatment with either ruxolitinib or fostamatinib significantly reduces the amount of IFN-β produced by Suit-2 cells in response to cellular infection by VSV. (D) Cellular

secretions were collected over the course of 48 h and cytokine production was measured by Verikine^{TM} IFN-Beta ELISA kit. There was no statistical difference between the amount of IFN-β between mock treated cells and VSV only treated cells. There was a significant difference in the amount of IFN-β of VSV only treated cells in comparison to both fostamatinib and ruxolitinib treated cells at 48 h p.i., with p-values of 0.0005 and <0.0001 respectively. (E) Cellular secretions from Suit-2 were collected over the course of 48 h and cytokine production was measured by Human IL-28A ELISA Kit. There was no statistical difference between the amount of IFN-λ between mock treated cells in comparison to either fostamatinib or ruxolitinib treated cells. There was a significant difference in the amount of IFN-λ of VSV only cells in comparison to both fostamatinib and ruxolitinib treated cells at both 24 and 48 h p.i., all of which were p-value <0.0001. (F) Cellular secretions from HPAF-II were collected over the course of 48 hours and cytokine production was measured by Human IL-28A ELISA Kit. There was no statistical difference between the amount of IFN-λ between mock treated cells in comparison to either fostamatinib or ruxolitinib treated cells. There was a significant difference in the amount of IFN-λ of VSV only cells in comparison to both fostamatinib and ruxolitinib treated cells at both 24 and 48 h p.i., all of which were p-value <0.0001. Treatment with either ruxolitinib or fostamatinib significantly reduces the amount of IFN-β produced by Suit-2 cells in response to cellular infection by VSV.

3.4 DISCUSSION

This compendium offers two distinct benefits, the first being the potential to find novel candidates for combinatorial treatment with VSV for OV as this is the first screening of its type with VSV. Second, it is important to know how any treatments or medications might impact clinical trials or OV treatment for patients once evaluation reaches that stage, and this table can also inform of drugs that may inhibit viral replication and oncolysis in addition to those that might stimulate viral replication, which is our primary interest.

We identified several promising FDA-approved drugs stimulating VSV replication to varying degrees across the range of PDAC cell lines, which did not exhibit cytotoxicity in non-malignant cells. Again, the limited number of effective treatments and increasing incidence of PDAC and other pancreatic tumors makes it absolutely imperative that we develop novel treatment options, especially those that are capable of improving efficacy in those tumors that are resistant to existing therapies. Interestingly, several commonly used pancreatic cancer chemotherapeutics were seemingly ineffective or even inhibited VSV replication in all five cell lines. Limitations in this approach were seen in consistency passing of the range of cell lines, the possibility of drug fluorescence, and the characteristics of viral replication in the cell lines.

From the initial library screening we determined that fostamatinib was capable of stimulating VSV replication in all PDAC cells lines, and that this reliably resulted in greater viral particle production, increased abundance of viral protein, and greater oncolytic activity. We hypothesized that, like ruxolitinib, the stimulation of viral replication was a result of inhibited antiviral signaling in the host cell. The indication that

both ruxolitinib and fostamatinib demonstrate similar levels of stimulation suggests that fostamatinib is likely inhibiting antiviral signaling within infected cells.

When we treated cells with exogenous IFN -α, STAT1 was clearly activated by phosphorylation in mock and fostamatinib treated cells, but was not detectable in ruxolitinib treated cells, as expected, and additional STAT2 phosphorylation in HPAF-II cells only, indicating that fostamatinib is not inhibiting Jak/STAT signaling directly. This also indicates that fostamatinib is not inhibiting type I IFN by the canonical pathway which means that viral stimulation must be a function of Syk inhibition or must be acting on type I IFNs downstream of Jak. When we looked at cytokine signaling in response to viral infection after treatment with fostamatinib, we saw that Syk inhibition prevented the production of IFN and the stimulation of ISGs in Suit-2 cells. We propose the possible mechanism of activity for fostamatinib-driven stimulation of viral replication is a result of inhibiting IFN signaling, resulting in downregulated STAT1 and STAT2 phosphorylation and inhibition of ISG expression, as demonstrated in Figure 13. This is a distinct mechanism from ruxolitinib, which directly inhibits Jak, preventing STAT1 and STAT2 phosphorylation even when IFN is present and interacting with IFNAR, which prevents the stimulation of ISGs within the cell.

Hypothetical Mechanism of Activity for Fostamatinib Driven Viral Stimulation

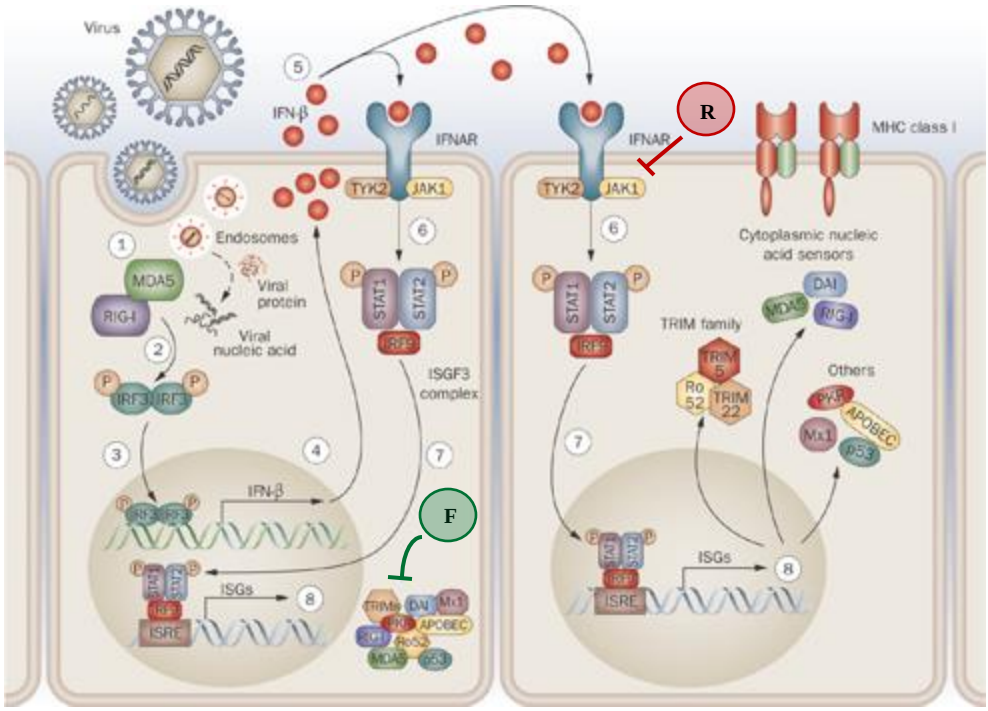

R Ruxolitinib – Jak Inhibitor F Fostamatinib – Syk Inhibitor

Figure 13. Hypothetical Mechanism of Activity. This figure shows our proposed mechanism of activity for fostamatinib.

While the absolute mechanism of activity is beyond the scope of this thesis, we do intend to determine whether fostamatinib is able or not to directly interact with Jak protein *in situ* and to confirm our hypothesis for the mechanism of activity. We also want to continue to evaluate the other candidate drugs identified in the library screening.

CHAPTER 4: CONCLUSION

As discussed previously, several factors pose a series of challenges that will determine whether OV is suitable for cancer treatment, especially for PDAC, where any treatment is further complicated by the TME, which is characterized by dense stroma comprised of abundant fibroblasts, hypoxia, sparse vasculature, as well as infiltration of tumor-promoting immune cells mediating immune evasion and tumor progression. The ideal OV treatment should allow for sufficient delivery and penetration of PDACs with the virus, induction of adaptive antitumor responses, and prevention of premature OV clearance by host antiviral response. It is unlikely that any monotherapy could address all these challenges, and future effective OV-based treatments will likely be combinatorial (chemo-virotherapy, radio-virotherapy, chemo-radio-virotherapy, chemo-radio-immuno-virotherapy, etc.). Many of VSV-based combinatorial approaches have been described in our previously published reviews (Felt and Grdzelishvili, 2017c; Hastie and Grdzelishvili, 2012b; Olagnier et al., 2017).

First of all, to study and address all these challenges, the ideal model systems should employ immunocompetent animals (to examine antiviral as well as antitumor immune responses) and be able to monitor not only tumor growth and spread, but also OV spread. PDAC is a highly heterogenic disease, and our studies have demonstrated dramatic differences between different human PDAC cell lines in their permissiveness to VSV and other OVs (Moerdyk-Schauwecker et al., 2013; Murphy et al., 2012b). Future studies should define distinct subtypes of PDACs to develop personalized treatment strategies for different types of PDACs (Collisson et al., 2011). Although there is still no consensus classification for clinical application, some treatments work better against a

particular PDAC subtype. For example, patients who had a germline BRCA mutation had significantly longer progression-free survival with maintenance a PARP inhibitor olaparib than with placebo. It could be interesting to test combinations of OVs with olaparib against PDACs that have the BRCAness phenotype (Wong et al., 2020). Interestingly, at least two studies showed the increased efficacy of OV therapy for thyroid carcinoma (Passaro et al., 2015) and glioblastoma (Zou et al., 2017) when OV was combined with olaparib.

Another major challenge for any PDAC treatment is insufficient drug delivery into the tumors because PDACs are hypovascular, densely packed with ECM components, have a high intratumoral tissue pressure, and very low tumor perfusion. Several previously developed approaches could be used to improve OV delivery into PDAC. For example, administration of a combination of cilengitide (angiogenesis inhibitor) and verapamil (Ca^{2+} channel blocker) promoted tumor angiogenesis, while improving gemcitabine delivery and therapeutic efficacy in mice. Additionally, the angiotensin inhibitor losartan was shown to increase perfusion, drug and oxygen delivery (Chauhan et al., 2013). A more recent study highlighted the potential importance of ROCK inhibition using the oral inhibitor fasudil for dual targeting of tumor tension and vasculature (Vennin et al., 2018). The administration of fasudil, a Rho-kinase inhibitor, and vasodilator, reduced intratumoral fibrillar collagen, improved sensitivity towards gemcitabine/nab-paclitaxel, and reduced metastasis formation on gemcitabine/abraxane treatment (Vennin et al., 2018). At least some of these drugs could potentially improve OV therapy when used in combination with VSV or other OVs.

The role of the stromal cells during OV therapy is still unclear, and it is likely dependent on the subtype of the particular PDAC. At least under certain conditions, the stromal cells could play a positive role during OV therapy by dampening antiviral responses within tumor and thus stimulating OV replication and OV-mediated oncolysis (Ilkow et al., 2015).

Other areas for development include approaches with a focus on antitumor immune stimulation. The TME of many cancers, including PDAC, is known to be immunosuppressive, due to various factors including a dense, fibrotic composition and a hypoxic environment that prevent access and activation of immune cells within the tumor (Bear et al., 2020; Morrison et al., 2018). Adoptive T-cell therapy augments the potency of T-cells by chaperoning virus into the tumor (Stevenson et al., 2000), overcoming the stromal barrier. Antigen-specific T-cells that were loaded with VSV-ΔM51 can also be used to produce viral infection, replication, and subsequent oncolysis, as well as producing a proinflammatory environment that helped suppress the immunosuppressive nature of the TME. Immune tolerance mechanisms have been implicated as the main barrier to effective antitumor immunotherapy (Wei et al., 2019), and the natural flora of the gut has been indicated to possess the ability to exert influence over the immune response of the TME, resulting in immune tolerance that promotes tumor growth and development.

In conclusion, we have conducted two independent multi-cell line screening of the complete FDA-approved drug library we have generated a table of the effects of drug treatments on VSV replication. Within these results we identified a novel candidate for potential combinatorial treatment with VSV-based oncolytic virotherapy. We confirmed

that fostamatinib works well to stimulate viral replication and subsequent oncolysis in all PDACs tested, even in cell lines resistant to VSV, without harming non-malignant cells. This activity is not limited to VSV, but is seen in other viruses as well, and evidence suggests that it is independent of Jak inhibition. Future experiments should examine the mechanism of activity for fostamatinib to determine whether it is eligible for preclinical evaluation as a combinatorial therapy with VSV *in vivo.* We also want to continue to evaluate the other candidate drugs identified in the library screening.

REFERENCES

Adamska, A., Elaskalani, O., Emmanouilidi, A., Kim, M., Abdol Razak, N.B., Metharom, P., Falasca, M., 2018. Molecular and cellular mechanisms of chemoresistance in pancreatic cancer. Adv Biol Regul 68, 77-87.

Ahmed, M., McKenzie, M.O., Puckett, S., Hojnacki, M., Poliquin, L., Lyles, D.S., 2003. Ability of the Matrix Protein of Vesicular Stomatitis Virus To Suppress Beta Interferon Gene Expression Is Genetically Correlated with the Inhibition of Host RNA and Protein Synthesis, J Virol, pp. 4646-4657.

Aier, I., Semwal, R., Sharma, A., Varadwaj, P.K., 2019. A systematic assessment of statistics, risk factors, and underlying features involved in pancreatic cancer. Cancer Epidemiol 58, 104-110.

Akakura, N., Kobayashi, M., Horiuchi, I., Suzuki, A., Wang, J., Chen, J., Niizeki, H., Kawamura, K., Hosokawa, M., Asaka, M., 2001. Constitutive expression of hypoxia-inducible factor-1alpha renders pancreatic cancer cells resistant to apoptosis induced by hypoxia and nutrient deprivation. Cancer Res 61, 6548-6554.

Amirache, F., Levy, C., Costa, C., Mangeot, P.E., Torbett, B.E., Wang, C.X., Negre, D., Cosset, F.L., Verhoeyen, E., 2014. Mystery solved: VSV-G-LVs do not allow efficient gene transfer into unstimulated T cells, B cells, and HSCs because they lack the LDL receptor. Blood 123, 1422-1424.

Ammayappan, A., Peng, K.W., Russell, S.J., 2013. Characteristics of oncolytic vesicular stomatitis virus displaying tumor-targeting ligands. J Virol 87, 13543-13555.

Amorino, G.P., Hamilton, V.M., Valerie, K., Dent, P., Lammering, G., Schmidt-Ullrich, R.K., 2002. Epidermal growth factor receptor dependence of radiation-induced transcription factor activation in human breast carcinoma cells. Mol Biol Cell 13, 2233-2244.

Ayala-Breton, C., Suksanpaisan, L., Mader, E.K., Russell, S.J., Peng, K.W., 2013. Amalgamating oncolytic viruses to enhance their safety, consolidate their killing mechanisms, and accelerate their spread. Mol Ther 21, 1930-1937.

Bafna, S., Kaur, S., Momi, N., Batra, S.K., 2009. Pancreatic cancer cells resistance to gemcitabine: the role of MUC4 mucin. Br J Cancer 101, 1155-1161.

Bailey, C.A., Miller, D.K., Lenard, J., 1984. Effects of DEAE-dextran on infection and hemolysis by VSV. Evidence that nonspecific electrostatic interactions mediate effective binding of VSV to cells. Virology 133, 111-118.

Balachandran, Barber, 2004. Defective Translational Control Facilitates Vesicular Stomatitis Virus Oncolysis. Cancer cell 5.

Barber, 2004. Vesicular Stomatitis Virus as an Oncolytic Vector. Viral immunology 17.

Bear, A.S., Vonderheide, R.H., O'Hara, M.H., 2020. Challenges and Opportunities for Pancreatic Cancer Immunotherapy. Cancer Cell 38, 788-802.

Black, B.L., Lyles, D.S., 1992. Vesicular stomatitis virus matrix protein inhibits host cell-directed transcription of target genes in vivo. J Virol 66, 4058-4064.

Black, B.L., Rhodes, R.B., McKenzie, M., Lyles, D.S., 1993. The role of vesicular stomatitis virus matrix protein in inhibition of host-directed gene expression is genetically separable from its function in virus assembly. J Virol 67, 4814-4821.

Bressy, C., Droby, G.N., Maldonado, B.D., Steuerwald, N., Grdzelishvili, V.Z., 2019. Cell Cycle Arrest in G2/M Phase Enhances Replication of Interferon-Sensitive Cytoplasmic RNA Viruses via Inhibition of Antiviral Gene Expression. J Virol 93.

Bressy, C., Hastie, E., Grdzelishvili, V.Z., 2017. Combining Oncolytic Virotherapy with p53 Tumor Suppressor Gene Therapy. Mol Ther Oncolytics 5, 20-40.

Brown, C.W., Stephenson, K.B., Hanson, S., Kucharczyk, M., Duncan, R., Bell, J.C., Lichty, B.D., 2009. The p14 FAST Protein of Reptilian Reovirus Increases Vesicular Stomatitis Virus Neuropathogenesis ▿ , J Virol, pp. 552-561.

Bukreyev, A., Skiadopoulos, M.H., Murphy, B.R., Collins, P.L., 2006. Nonsegmented negative-strand viruses as vaccine vectors. J Virol 80, 10293-10306.

Buscail, L., Bournet, B., Cordelier, P., 2020. Role of oncogenic KRAS in the diagnosis, prognosis and treatment of pancreatic cancer. Nat Rev Gastroenterol Hepatol 17, 153-168.

Carneiro, F.A., Lapido-Loureiro, P.A., Cordo, S.M., Stauffer, F., Weissmuller, G., Bianconi, M.L., Juliano, M.A., Juliano, L., Bisch, P.M., Da Poian, A.T., 2006. Probing the interaction between vesicular stomatitis virus and phosphatidylserine. Eur Biophys J 35, 145-154.

Cataldi, M., Shah, N.R., Felt, S.A., Grdzelishvili, V.Z., 2015. Breaking resistance of pancreatic cancer cells to an attenuated vesicular stomatitis virus through a novel activity of IKK inhibitor TPCA-1. Virology 485, 340-354.

Chad A Barnes, M.I.C., Susan Tsai, Mohammed Aldakkak, Ben George, Paul S Ritch, Kulwinder Dua, Callisia N Clarke, Parag Tolat, Catherine Hagen, William A Hall, Beth A Erickson, Douglas B Evans, Kathleen K Christians, 2019. Survival of patients with borderline resectable pancreatic cancer who received neoadjuvant therapy and surgery. Surgery.

Chang, K.J., Senzer, N.N., Binmoeller, K., Goldsweig, H., Coffin, R., 2012. Phase I dose-escalation study of talimogene laherparepvec (T-VEC) for advanced pancreatic cancer (ca). 30, e14546-e14546.

Chauhan, V.P., Martin, J.D., Liu, H., Lacorre, D.A., Jain, S.R., Kozin, S.V., Stylianopoulos, T., Mousa, A.S., Han, X., Adstamongkonkul, P., Popovic, Z., Huang, P., Bawendi, M.G., Boucher, Y., Jain, R.K., 2013. Angiotensin inhibition enhances drug delivery and potentiates chemotherapy by decompressing tumour blood vessels. Nat Commun 4, 2516.

Chen, W., Fan, W., Ru, G., Huang, F., Lu, X., Zhang, X., Mou, X., Wang, S., 2019. Gemcitabine combined with an engineered oncolytic vaccinia virus exhibits a synergistic suppressive effect on the tumor growth of pancreatic cancer. Oncol Rep 41, 67-76.

Cicenas, J., Kvederaviciute, K., Meskinyte, I., Meskinyte-Kausiliene, E., Skeberdyte, A., Cicenas, J., 2017. KRAS, TP53, CDKN2A, SMAD4, BRCA1, and BRCA2 Mutations in Pancreatic Cancer. Cancers (Basel) 9.

Clarke DK, N.F., Lee M, Johnson JE, Wright K, Calderon P, Guo M, Natuk R, Cooper D, Hendry RM, Udem SA., 2007. Synergistic attenuation of vesicular stomatitis virus by combination of specific G gene truncations and N gene translocations. Journal of Virology 81, 2056-2064.

Coil, D.A., Miller, A.D., 2004. Phosphatidylserine is not the cell surface receptor for vesicular stomatitis virus. J Virol 78, 10920-10926.

Collisson, E.A., Sadanandam, A., Olson, P., Gibb, W.J., Truitt, M., Gu, S., Cooc, J., Weinkle, J., Kim, G.E., Jakkula, L., Feiler, H.S., Ko, A.H., Olshen, A.B., Danenberg, K.L., Tempero, M.A., Spellman, P.T., Hanahan, D., Gray, J.W., 2011. Subtypes of pancreatic ductal adenocarcinoma and their differing responses to therapy. Nat Med 17, 500-503.

Conti, C., Mastromarino, P., Riccioli, A., Orsi, N., 1991. Electrostatic interactions in the early events of VSV infection. Res Virol 142, 17-24.

Coulon, Deutsch, Lafay, Martinet-Edelist, Wyers, Herman, Flamand, 1990. Genetic Evidence for Multiple Functions of the Matrix Protein of Vesicular Stomatitis Virus. The Journal of general virology 71 (Pt 4).

Daisuke Uchida 1, H.S., Hironari Kato, Teruya Nagahara, Masaya Iwamuro, Junro Kataoka, Shigeru Horiguchi, Masami Watanabe, Akinobu Takaki, Kazuhiro Nouso, Yasutomo Nasu, Takahito Yagi, Hiromi Kumon, Kazuhide Yamamoto, 2014. Potential of adenovirus-mediated REIC/Dkk-3 gene therapy for use in the treatment of pancreatic cancer. Journal of Gastroenterol Hepatology 29.

Dang, C.V., 2017. MUC-king with HIF May Rewire Pyrimidine Biosynthesis and Curb Gemcitabine Resistance in Pancreatic Cancer. Cancer Cell 32, 3-5.

Dauer, P., Nomura, A., Saluja, A., Banerjee, S., 2017. Microenvironment in determining chemo-resistance in pancreatic cancer: Neighborhood matters. Pancreatology 17, 7-12.

Deer, E.L., Gonzalez-Hernandez, J., Coursen, J.D., Shea, J.E., Ngatia, J., Scaife, C.L., Firpo, M.A., Mulvihill, S.J., 2010. Phenotype and genotype of pancreatic cancer cell lines. Pancreas 39, 425-435.

Ebert, Harbaran, Shinozaki, Woo, 2005. Systemic Therapy of Experimental Breast Cancer Metastases by Mutant Vesicular Stomatitis Virus in Immune-Competent Mice. Cancer gene therapy 12.

Eisenberg, D.P., Adusumilli, P.S., Hendershott, K.J., Yu, Z., Mullerad, M., Chan, M.K., Chou, T.C., Fong, Y., 2005. 5-fluorouracil and gemcitabine potentiate the efficacy of oncolytic herpes viral gene therapy in the treatment of pancreatic cancer. J Gastrointest Surg 9, 1068-1077; discussion 1077-1069.

Eissa, I.R., Bustos-Villalobos, I., Ichinose, T., Matsumura, S., Naoe, Y., Miyajima, N., Morimoto, D., Mukoyama, N., Zhiwen, W., Tanaka, M., Hasegawa, H., Sumigama, S., Aleksic, B., Kodera, Y., Kasuya, H., 2018. The Current Status and Future Prospects of Oncolytic Viruses in Clinical Trials against Melanoma, Glioma, Pancreatic, and Breast Cancers. Cancers (Basel) 10.

Felt, S.A., Droby, G.N., Grdzelishvili, V.Z., 2017. Ruxolitinib and Polycation Combination Treatment Overcomes Multiple Mechanisms of Resistance of Pancreatic Cancer Cells to Oncolytic Vesicular Stomatitis Virus. J Virol 91.

Felt, S.A., Grdzelishvili, V.Z., 2017a. Recent advances in vesicular stomatitis virus-based oncolytic virotherapy: a 5-year update. Journal of General Virology 98, 2895-2911.

Felt, S.A., Grdzelishvili, V.Z., 2017b. Recent advances in vesicular stomatitis virus-based oncolytic virotherapy: a 5-year update, J Gen Virol, pp. 2895-2911.

Felt, S.A., Grdzelishvili, V.Z., 2017c. Recent advances in vesicular stomatitis virus-based oncolytic virotherapy: a 5-year update. J Gen Virol 98, 2895-2911.

Felt, S.A., Moerdyk-Schauwecker, M.J., Grdzelishvili, V.Z., 2015. Induction of apoptosis in pancreatic cancer cells by vesicular stomatitis virus. Virology 474, 163-173.

Finkelshtein, D., Werman, A., Novick, D., Barak, S., Rubinstein, M., 2013. LDL receptor and its family members serve as the cellular receptors for vesicular stomatitis virus. Proc Natl Acad Sci USA 110, 7306-7311.

Freedman, J.D., Duffy, M.R., Lei-Rossmann, J., Muntzer, A., Scott, E.M., Hagel, J., Campo, L., Bryant, R.J., Verrill, C., Lambert, A., Miller, P., Champion, B.R., Seymour, L.W., Fisher, K.D., 2018. An Oncolytic Virus Expressing a T-cell Engager Simultaneously Targets Cancer and Immunosuppressive Stromal Cells. Cancer Res 78, 6852-6865.

Froeling, F.E., Marshall, J.F., Kocher, H.M., 2010. Pancreatic cancer organotypic cultures. J Biotechnol 148, 16-23.

Gaddy, Lyles, 2007. Oncolytic vesicular stomatitis virus induces apoptosis via signaling through PKR, Fas, and Daxx. Journal of virology 81.

Gidekel Friedlander, S.Y., Chu, G.C., Snyder, E.L., Girnius, N., Dibelius, G., Crowley, D., Vasile, E., DePinho, R.A., Jacks, T., 2009. Context-dependent transformation of adult pancreatic cells by oncogenic K-Ras. Cancer Cell 16, 379-389.

Gillet, J.P., Varma, S., Gottesman, M.M., 2013. The clinical relevance of cancer cell lines. J Natl Cancer Inst 105, 452-458.

Giovannetti, E., Del Tacca, M., Mey, V., Funel, N., Nannizzi, S., Ricci, S., Orlandini, C., Boggi, U., Campani, D., Del Chiaro, M., Iannopollo, M., Bevilacqua, G., Mosca, F., Danesi, R., 2006. Transcription analysis of human equilibrative nucleoside transporter-1 predicts survival in pancreas cancer patients treated with gemcitabine. Cancer Res 66, 3928-3935.

Guibinga, G.H., Miyanohara, A., Esko, J.D., Friedmann, T., 2002. Cell surface heparan sulfate is a receptor for attachment of envelope protein-free retrovirus-like particles and VSV-G pseudotyped MLV-derived retrovirus vectors to target cells. Mol Ther 5, 538-546.

Hastie, E., Besmer, D.M., Shah, N.R., Murphy, A.M., Moerdyk-Schauwecker, M., Molestina, C., Roy, L.D., Curry, J.M., Mukherjee, P., Grdzelishvili, V.Z., 2013a. Oncolytic vesicular stomatitis virus in an immunocompetent model of MUC1-positive or MUC1-null pancreatic ductal adenocarcinoma. J Virol 87, 10283-10294.

Hastie, E., Cataldi, M., Marriott, I., Grdzelishvili, V.Z., 2013b. Understanding and altering cell tropism of vesicular stomatitis virus. Virus Res 176.

Hastie, E., Cataldi, M., Moerdyk-Schauwecker, M.J., Felt, S.A., Steuerwald, N., Grdzelishvili, V.Z., 2016. Novel biomarkers of resistance of pancreatic cancer cells to oncolytic vesicular stomatitis virus. Oncotarget 7, 61601-61618.

Hastie, E., Cataldi, M., Steuerwald, N., Grdzelishvili, V.Z., 2015. An unexpected inhibition of antiviral signaling by virus-encoded tumor suppressor p53 in pancreatic cancer cells. Virology 483, 126-140.

Hastie, E., Grdzelishvili, V.Z., 2012a. Vesicular stomatitis virus as a flexible platform for oncolytic virotherapy against cancer. J Gen Virol 93, 2529-2545.

Hastie, E., Grdzelishvili, V.Z., 2012b. Vesicular stomatitis virus as a flexible platform for oncolytic virotherapy against cancer, J Gen Virol, pp. 2529-2545.

Hecht, J.R., Bedford, R., Abbruzzese, J.L., Lahoti, S., Reid, T.R., Soetikno, R.M., Kirn, D.H., Freeman, S.M., 2003. A phase I/II trial of intratumoral endoscopic ultrasound injection of ONYX-015 with intravenous gemcitabine in unresectable pancreatic carcinoma. Clin Cancer Res 9, 555-561.

Heiber, J.F., Barber, G.N., 2011. Vesicular stomatitis virus expressing tumor suppressor p53 is a highly attenuated, potent oncolytic agent. J Virol 85, 10440-10450.

Hirooka, Y., Kasuya, H., Ishikawa, T., Kawashima, H., Ohno, E., Villalobos, I.B., Naoe, Y., Ichinose, T., Koyama, N., Tanaka, M., Kodera, Y., Goto, H., 2018. A Phase I clinical trial of EUS-guided intratumoral injection of the oncolytic virus, HF10 for unresectable locally advanced pancreatic cancer. BMC Cancer 18, 596.

Holbrook, M.C., Goad, D.W., Grdzelishvili, V.Z., 2021. Expanding the Spectrum of Pancreatic Cancers Responsive to Vesicular Stomatitis Virus-Based Oncolytic Virotherapy: Challenges and Solutions. Cancers (Basel) 13.

Ilkow, C.S., Marguerie, M., Batenchuk, C., Mayer, J., Ben Neriah, D., Cousineau, S., Falls, T., Jennings, V.A., Boileau, M., Bellamy, D., Bastin, D., de Souza, C.T., Alkayyal, A., Zhang, J., Le Boeuf, F., Arulanandam, R., Stubbert, L., Sampath, P., Thorne, S.H., Paramanthan, P., Chatterjee, A., Strieter, R.M., Burdick, M., Addison, C.L., Stojdl, D.F., Atkins, H.L., Auer, R.C., Diallo, J.S., Lichty, B.D., Bell, J.C., 2015. Reciprocal cellular cross-talk within the tumor microenvironment promotes oncolytic virus activity. Nat Med 21, 530-536.

Ireland, L., Santos, A., Ahmed, M.S., Rainer, C., Nielsen, S.R., Quaranta, V., Weyer-Czernilofsky, U., Engle, D.D., Perez-Mancera, P.A., Coupland, S.E., Taktak, A., Bogenrieder, T., Tuveson, D.A., Campbell, F., Schmid, M.C., Mielgo, A., 2016. Chemoresistance in Pancreatic Cancer Is Driven by Stroma-Derived Insulin-Like Growth Factors. Cancer Res 76, 6851-6863.

Johnson JE, Nasar F, Coleman JW, Price RE, Javadian A, Draper K, Lee M, Reilly PA, Clarke DK, Hendry RM, Udem, S.A., 2007. Neurovirulence properties of recombinant vesicular stomatitis virus vectors in non-human primates. Virology 360, 36-49.

Kalra, A.V., Campbell, R.B., 2007. Mucin impedes cytotoxic effect of 5-FU against growth of human pancreatic cancer cells: overcoming cellular barriers for therapeutic gain. Br J Cancer 97, 910-918.

Kamisawa, T., Wood, Laura D, Itoi, Takao, and Takaori, Kyoichi, 2016. Pancreatic Cancer. The Lancet 388, 73-85.

Kasuya, K., Tsuchida, A., Nagakawa, Y., Suzuki, M., Abe, Y., Itoi, T., Serizawa, H., Nagao, T., Shimazu, M., Aoki, T., 2011. Hypoxia-inducible factor-1alpha expression and gemcitabine chemotherapy for pancreatic cancer. Oncol Rep 26, 1399-1406.

Ke, J., Peng, X., Mei, S., Tian, J., Ying, P., Yang, N., Wang, X., Zou, D., Yang, Y., Zhu, Y., Gong, Y., Gong, J., Zhong, R., Chang, J., Fang, Z., Miao, X., 2020. Evaluation of polymorphisms in microRNA-binding sites and pancreatic cancer risk in Chinese population. J Cell Mol Med 24, 2252-2259.

Kelly, E., Russell, S.J., 2007. History of oncolytic viruses: genesis to genetic engineering. Molecular therapy : the journal of the American Society of Gene Therapy 15, 651-659.

Khodarev, N.N., Beckett, M., Labay, E., Darga, T., Roizman, B., Weichselbaum, R.R., 2004. STAT1 is overexpressed in tumors selected for radioresistance and confers protection from radiation in transduced sensitive cells, Proc Natl Acad Sci U S A, pp. 1714-1719.

Kleeff, J., Beckhove, P., Esposito, I., Herzig, S., Huber, P.E., Lohr, J.M., Friess, H., 2007. Pancreatic cancer microenvironment. Int J Cancer 121, 699-705.

Kobbe, v., Deursen, v., Rodrigues, Sitterlin, Bachi, Wu, Wilm, Carmo-Fonseca, Izaurralde, 2000. Vesicular Stomatitis Virus Matrix Protein Inhibits Host Cell Gene Expression by Targeting the Nucleoporin Nup98. Molecular cell 6.

Kohei Horioka 1, K.O., Masafumi Sada 1, Biao Zheng 1, Taiki Moriyama 1, Hayato Fujita 1, Tatsuya Manabe 1, Takao Ohtsuka 1, Masaya Shimamoto 2, Tetsuyuki Miyazaki 1, Kazuhiro Mizumoto 2, Yoshinao Oda 3, Masafumi Nakamura 1, 2016. Suppression of CD51 in pancreatic stellate cells inhibits tumor growth by reducing stroma and altering tumor-stromal interaction in pancreatic cancer. International journal of oncology.

Lambert, P.F., Banks, L., 2019. Human tumour viruses, in: Baan, R.A., Stewart, B.W., Straif, K. (Eds.), Tumour Site Concordance and Mechanisms of Carcinogenesis, Lyon (FR).

Lee, J.C., Shin, D.W., Park, H., Kim, J., Youn, Y., Kim, J.H., Kim, J., Hwang, J.H., 2020. Tolerability and safety of EUS-injected adenovirus-mediated double-suicide gene therapy with chemotherapy in locally advanced pancreatic cancer: a phase 1 trial. Gastrointest Endosc 92, 1044-1052 e1041.

Letchworth, G.J., Rodriguez, L.L., Del cbarrera, J., 1999. Vesicular stomatitis. The Veterinary Journal 157, 239-260.

Li, Q., Tainsky, M.A., 2011. Epigenetic silencing of IRF7 and/or IRF5 in lung cancer cells leads to increased sensitivity to oncolytic viruses. PLoS One 6, e28683.

Lichty, Power, Stojdl, Bell, 2004. Vesicular Stomatitis Virus: Re-Inventing the Bullet. Trends in molecular medicine 10.

Liu, S., Liao, Y., Chen, B., Chen, Y., Yu, Z., Wei, H., Zhang, L., Huang, S., Rothman, P.B., Gao, G.F., Chen, J.L., 2021. Critical role of Syk-dependent STAT1 activation in innate antiviral immunity. Cell Rep 34, 108627.

Mahalingam, D., Wilkinson, G.A., Eng, K.H., Fields, P., Raber, P., Moseley, J.L., Cheetham, K., Coffey, M., Nuovo, G., Kalinski, P., Zhang, B., Arora, S.P., Fountzilas, C., 2020. Pembrolizumab in Combination with the Oncolytic Virus Pelareorep and Chemotherapy in Patients with Advanced Pancreatic Adenocarcinoma: A Phase Ib Study. Clin Cancer Res 26, 71-81.

Marozin, S., Altomonte, J., Stadler, F., Thasler, W.E., Schmid, R.M., Ebert, O., 2008. Inhibition of the IFN-beta Response in Hepatocellular Carcinoma by Alternative Spliced Isoform of IFN Regulatory Factor-3. Mol Ther 16, 1789-1797.

Marozin, S., De Toni, E.N., Rizzani, A., Altomonte, J., Junger, A., Schneider, G., Thasler, W.E., Kato, N., Schmid, R.M., Ebert, O., 2010. Cell Cycle Progression or Translation Control Is Not Essential for Vesicular Stomatitis Virus Oncolysis of Hepatocellular Carcinoma, PLoS One.

McGuigan, A., Kelly, P., Turkington, R.C., Jones, C., Coleman, H.G., McCain, R.S., 2018. Pancreatic cancer: A review of clinical diagnosis, epidemiology, treatment and outcomes. World J Gastroenterol 24, 4846-4861.

Mimeault, M., Johansson, S.L., Senapati, S., Momi, N., Chakraborty, S., Batra, S.K., 2010. MUC4 down-regulation reverses chemoresistance of pancreatic cancer stem/progenitor cells and their progenies. Cancer Lett 295, 69-84.

Moehler, M., Sieben, M., Roth, S., Springsguth, F., Leuchs, B., Zeidler, M., Dinsart, C., Rommelaere, J., Galle, P.R., 2011. Activation of the human immune system by chemotherapeutic or targeted agents combined with the oncolytic parvovirus H-1. BMC Cancer 11, 464.

Moerdyk-Schauwecker, M., Shah, N.R., Murphy, A.M., Hastie, E., Mukherjee, P., Grdzelishvili, V.Z., 2013. Resistance of pancreatic cancer cells to oncolytic vesicular stomatitis virus: role of type I interferon signaling. Virology 436, 221-234.

Monsurro, V., Beghelli, S., Wang, R., Barbi, S., Coin, S., Di Pasquale, G., Bersani, S., Castellucci, M., Sorio, C., Eleuteri, S., Worschech, A., Chiorini, J.A., Pederzoli, P., Alter, H., Marincola, F.M., Scarpa, A., 2010. Anti-viral state segregates two molecular phenotypes of pancreatic adenocarcinoma: potential relevance for adenoviral gene therapy. J Transl Med 8, 10.

Morrison, A.H., Byrne, K.T., Vonderheide, R.H., 2018. Immunotherapy and Prevention of Pancreatic Cancer. Trends Cancer 4, 418-428.

Moussavi, M., Fazli, L., Tearle, H., Guo, Y., Cox, M., Bell, J., Ong, C., Jia, W., Rennie, P.S., 2010. Oncolysis of prostate cancers induced by vesicular stomatitis virus in PTEN knockout mice. Cancer Res 70, 1367-1376.

Mulvihill, S., Warren, R., Venook, A., Adler, A., Randlev, B., Heise, C., Kirn, D., 2001. Safety and feasibility of injection with an E1B-55 kDa gene-deleted, replication-selective adenovirus (ONYX-015) into primary carcinomas of the pancreas: a phase I trial. Gene Ther 8, 308-315.

Murphy, A.M., Besmer, D.M., Moerdyk-Schauwecker, M., Moestl, N., Ornelles, D.A., Mukherjee, P., Grdzelishvili, V.Z., 2012a. Vesicular Stomatitis Virus as an Oncolytic Agent against Pancreatic Ductal Adenocarcinoma, J Virol, pp. 3073-3087.

Murphy, A.M., Besmer, D.M., Moerdyk-Schauwecker, M., Moestl, N., Ornelles, D.A., Mukherjee, P., Grdzelishvili, V.Z., 2012b. Vesicular stomatitis virus as an oncolytic agent against pancreatic ductal adenocarcinoma. J Virol 86, 3073-3087.

Mutgan, A.C., Besikcioglu, H.E., Wang, S., Friess, H., Ceyhan, G.O., Demir, I.E., 2018. Insulin/IGF-driven cancer cell-stroma crosstalk as a novel therapeutic target in pancreatic cancer. Mol Cancer 17, 66.

Nath, S., Daneshvar, K., Roy, L.D., Grover, P., Kidiyoor, A., Mosley, L., Sahraei, M., Mukherjee, P., 2013. MUC1 induces drug resistance in pancreatic cancer cells via upregulation of multidrug resistance genes. Oncogenesis 2, e51.

Nikolic, J., Belot, L., Raux, H., Legrand, P., Gaudin, Y., A, A.A., 2018. Structural basis for the recognition of LDL-receptor family members by VSV glycoprotein. Nat Commun 9, 1029.

Nishimoto, T., Yoshida, K., Miura, Y., Kobayashi, A., Hara, H., Ohnami, S., Kurisu, K., Yoshida, T., Aoki, K., 2009. Oncolytic virus therapy for pancreatic cancer using the adenovirus library displaying random peptides on the fiber knob. Gene Ther 16, 669-680.

Noser, J.A., Mael, A.A., Sakuma, R., Ohmine, S., Marcato, P., Lee, P.W., Ikeda, Y., 2007. The RAS/Raf1/MEK/ERK signaling pathway facilitates VSV-mediated oncolysis: implication for the defective interferon response in cancer cells. Mol Ther 15, 1531-1536.

Ohhashi, S., Ohuchida, K., Mizumoto, K., Fujita, H., Egami, T., Yu, J., Toma, H., Sadatomi, S., Nagai, E., Tanaka, M., 2008. Down-regulation of deoxycytidine kinase enhances acquired resistance to gemcitabine in pancreatic cancer. Anticancer Res 28, 2205-2212.

Olagnier, D., Lababidi, R.R., Hadj, S.B., Sze, A., Liu, Y., Naidu, S.D., Ferrari, M., Jiang, Y., Chiang, C., Beljanski, V., Goulet, M.L., Knatko, E.V., Dinkova-Kostova, A.T., Hiscott, J., Lin, R., 2017. Activation of Nrf2 Signaling Augments Vesicular Stomatitis Virus Oncolysis via Autophagy-Driven Suppression of Antiviral Immunity. Mol Ther 25, 1900-1916.

Parekh, H.D., Starr, J., George, T.J., Jr., 2017. The Multidisciplinary Approach to Localized Pancreatic Adenocarcinoma. Curr Treat Options Oncol 18, 73.

Passaro, C., Volpe, M., Botta, G., Scamardella, E., Perruolo, G., Gillespie, D., Libertini, S., Portella, G., 2015. PARP inhibitor olaparib increases the oncolytic activity of dl922-947 in in vitro and in vivo model of anaplastic thyroid carcinoma. Mol Oncol 9, 78-92.

Perri, G., Prakash, L., Katz, M.H.G., 2020. Defining and Treating Borderline Resectable Pancreatic Cancer. Curr Treat Options Oncol 21, 71.

Petersen, J.M., Her, L.S., Varvel, V., Lund, E., Dahlberg, J.E., 2000. The matrix protein of vesicular stomatitis virus inhibits nucleocytoplasmic transport when it is in the nucleus

and associated with nuclear pore complexes. Molecular and cellular biology 20, 8590-8601.

Quillien, L., Top, S., Kappler-Gratias, S., Redoute, A., Dusetti, N., Quentin-Froignant, C., Lulka, H., Camus-Bouclainville, C., Buscail, L., Gallardo, F., Bertagnoli, S., Cordelier, P., 2021. A Novel Imaging Approach for Single-Cell Real-Time Analysis of Oncolytic Virus Replication and Efficacy in Cancer Cells. Hum Gene Ther 32, 166-177.

Rodriguez-Garcia, A., Gimenez-Alejandre, M., Rojas, J.J., Moreno, R., Bazan-Peregrino, M., Cascallo, M., Alemany, R., 2015. Safety and efficacy of VCN-01, an oncolytic adenovirus combining fiber HSG-binding domain replacement with RGD and hyaluronidase expression. Clin Cancer Res 21, 1406-1418.

Rouanet, M., Lebrin, M., Gross, F., Bournet, B., Cordelier, P., Buscail, L., 2017. Gene Therapy for Pancreatic Cancer: Specificity, Issues and Hopes. Int J Mol Sci 18.

Russell L, P.K., Russell SJ, and Diaz RM, 2019. Oncolytic Viruses: Priming Time for Cancer Immunotherapy. BioDrugs 33, 485-501.

Russell, S.J., Peng, K.W., Bell, J.C., 2012. Oncolytic virotherapy. Nat Biotechnol 30, 658-670.

Saiki, Y., Yoshino, Y., Fujimura, H., Manabe, T., Kudo, Y., Shimada, M., Mano, N., Nakano, T., Lee, Y., Shimizu, S., Oba, S., Fujiwara, S., Shimizu, H., Chen, N., Nezhad, Z.K., Jin, G., Fukushige, S., Sunamura, M., Ishida, M., Motoi, F., Egawa, S., Unno, M., Horii, A., 2012. DCK is frequently inactivated in acquired gemcitabine-resistant human cancer cells. Biochem Biophys Res Commun 421, 98-104.

Salo-Mullen, E.E., O'Reilly, E.M., Kelsen, D.P., Ashraf, A.M., Lowery, M.A., Yu, K.H., Reidy, D.L., Epstein, A.S., Lincoln, A., Saldia, A., Jacobs, L.M., Rau-Murthy, R., Zhang, L., Kurtz, R.C., Saltz, L., Offit, K., Robson, M.E., Stadler, Z.K., 2015. Identification of germline genetic mutations in patients with pancreatic cancer. Cancer 121, 4382-4388.

Sato-Dahlman, M., Yamamoto, M., 2018. The Development of Oncolytic Adenovirus Therapy in the Past and Future - For the Case of Pancreatic Cancer. Curr Cancer Drug Targets 18, 153-161.

Schlegel, R., Tralka, T.S., Willingham, M.C., Pastan, I., 1983. Inhibition of VSV binding and infectivity by phosphatidylserine: is phosphatidylserine a VSV-binding site? Cell 32, 639-646.

Schloemer, R.H., Wagner, R.R., 1975. Cellular adsorption function of the sialoglycoprotein of vesicular stomatitis virus and its neuraminic acid. J Virol 15, 882-893.

Seegers, S.L., Frasier, C., Greene, S., Nesmelova, I.V., Grdzelishvili, V.Z., 2020. Experimental Evolution Generates Novel Oncolytic Vesicular Stomatitis Viruses with Improved Replication in Virus-Resistant Pancreatic Cancer Cells. J Virol 94.

Shindo, K., Yu, J., Suenaga, M., Fesharakizadeh, S., Cho, C., Macgregor-Das, A., Siddiqui, A., Witmer, P.D., Tamura, K., Song, T.J., Navarro Almario, J.A., Brant, A., Borges, M., Ford, M., Barkley, T., He, J., Weiss, M.J., Wolfgang, C.L., Roberts, N.J., Hruban, R.H., Klein, A.P., Goggins, M., 2017. Deleterious Germline Mutations in Patients With Apparently Sporadic Pancreatic Adenocarcinoma. J Clin Oncol 35, 3382-3390.

Shukla, S.K., Purohit, V., Mehla, K., Gunda, V., Chaika, N.V., Vernucci, E., King, R.J., Abrego, J., Goode, G.D., Dasgupta, A., Illies, A.L., Gebregiworgis, T., Dai, B., Augustine, J.J., Murthy, D., Attri, K.S., Mashadova, O., Grandgenett, P.M., Powers, R., Ly, Q.P., Lazenby, A.J., Grem, J.L., Yu, F., Mates, J.M., Asara, J.M., Kim, J.W., Hankins, J.H., Weekes, C., Hollingsworth, M.A., Serkova, N.J., Sasson, A.R., Fleming, J.B., Oliveto, J.M., Lyssiotis, C.A., Cantley, L.C., Berim, L., Singh, P.K., 2017. MUC1 and HIF-1alpha Signaling Crosstalk Induces Anabolic Glucose Metabolism to Impart Gemcitabine Resistance to Pancreatic Cancer. Cancer Cell 32, 392.

Siegel, R.L., Miller, Kimberly D, and Jemal, Ahmedin, 2020. Cancer Facts & Figures 2020. CA: A Cancer Journal for Clinicians 70.

Simovic, B., Walsh, S.R., Wan, Y., 2015. Mechanistic insights into the oncolytic activity of vesicular stomatitis virus in cancer immunotherapy, Oncolytic Virother, pp. 157-167.

Skrypek, N., Duchene, B., Hebbar, M., Leteurtre, E., van Seuningen, I., Jonckheere, N., 2013. The MUC4 mucin mediates gemcitabine resistance of human pancreatic cancer cells via the Concentrative Nucleoside Transporter family. Oncogene 32, 1714-1723.

Spratlin, J., Sangha, R., Glubrecht, D., Dabbagh, L., Young, J.D., Dumontet, C., Cass, C., Lai, R., Mackey, J.R., 2004. The absence of human equilibrative nucleoside transporter 1 is associated with reduced survival in patients with gemcitabine-treated pancreas adenocarcinoma. Clin Cancer Res 10, 6956-6961.

Springfeld, C., Jager, D., Buchler, M.W., Strobel, O., Hackert, T., Palmer, D.H., Neoptolemos, J.P., 2019. Chemotherapy for pancreatic cancer. Presse Med 48, e159-e174.

Steinhauer, D.A., Domingo, E., Holland, J.J., 1992. Lack of evidence for proofreading mechanisms associated with an RNA virus polymerase. Gene 122, 281-288.

Stevenson, A.J., Giles, M.S., Hall, K.T., Goodwin, D.J., Calderwood, M.A., Markham, A.F., Whitehouse, A., 2000. Specific oncolytic activity of herpesvirus saimiri in pancreatic cancer cells. Br J Cancer 83, 329-332.

Stojdl, Lichty, Knowles, Marius, Atkins, Sonenberg, Bell, 2000. Exploiting Tumor-Specific Defects in the Interferon Pathway With a Previously Unknown Oncolytic Virus. Nature medicine 6.

Stojdl, Lichty, tenOever, Paterson, Power, Knowles, Marius, Reynard, Poliquin, Atkins, Brown, Durbin, Durbin, Hiscott, Bell, 2003. VSV Strains With Defects in Their Ability to Shutdown Innate Immunity Are Potent Systemic Anti-Cancer Agents. Cancer cell 4.

Tesh, R.B., Peralta, P.H., Johnson, K.M., 1969. Ecologic studies of vesicular stomatitis virus. I. Prevalence of infection among animals and humans living in an area of endemic VSV activity. Am J Epidemiol 90, 255-261.

Torres, M.P., Rachagani, S., Souchek, J.J., Mallya, K., Johansson, S.L., Batra, S.K., 2013. Novel pancreatic cancer cell lines derived from genetically engineered mouse models of spontaneous pancreatic adenocarcinoma: applications in diagnosis and therapy. PLoS One 8, e80580.

Trehoux, S., Duchene, B., Jonckheere, N., Van Seuningen, I., 2015. The MUC1 oncomucin regulates pancreatic cancer cell biological properties and chemoresistance. Implication of p42-44 MAPK, Akt, Bcl-2 and MMP13 pathways. Biochem Biophys Res Commun 456, 757-762.

Trottier, M.D., Lyles, D.S., Reiss, C.S., 2007. Peripheral, but not central nervous system, type I interferon expression in mice in response to intranasal vesicular stomatitis virus infection. J Neurovirol 13, 433-445.

Turpin, A., El Amrani, M., Bachet, J.B., Pietrasz, D., Schwarz, L., Hammel, P., 2020. Adjuvant Pancreatic Cancer Management: Towards New Perspectives in 2021. Cancers (Basel) 12.

Tysome, J.R., Briat, A., Alusi, G., Cao, F., Gao, D., Yu, J., Wang, P., Yang, S., Dong, Z., Wang, S., Deng, L., Francis, J., Timiryasova, T., Fodor, I., Lemoine, N.R., Wang, Y., 2009. Lister strain of vaccinia virus armed with endostatin-angiostatin fusion gene as a novel therapeutic agent for human pancreatic cancer. Gene Ther 16, 1223-1233.

Vennin, C., Murphy, K.J., Morton, J.P., Cox, T.R., Pajic, M., Timpson, P., 2018. Reshaping the Tumor Stroma for Treatment of Pancreatic Cancer. Gastroenterology 154, 820-838.

Vernejoul, F., Ghenassia, L., Souque, A., Lulka, H., Drocourt, D., Cordelier, P., Pradayrol, L., Pyronnet, S., Buscail, L., Tiraby, G., 2006. Gene therapy based on gemcitabine chemosensitization suppresses pancreatic tumor growth. Mol Ther 14, 758-767.

Wang, Rahbar, Fish, 2011. Interferon: Current Status and Future Prospects in Cancer Therapy. Journal of interferon & cytokine research : the official journal of the International Society for Interferon and Cytokine Research 31.

Wang, S., You, L., Dai, M., Zhao, Y., 2020. Mucins in pancreatic cancer: A well-established but promising family for diagnosis, prognosis and therapy. J Cell Mol Med 24, 10279-10289.

Wei, M.Y., Shi, S., Liang, C., Meng, Q.C., Hua, J., Zhang, Y.Y., Liu, J., Zhang, B., Xu, J., Yu, X.J., 2019. The microbiota and microbiome in pancreatic cancer: more influential than expected. Mol Cancer 18, 97.

Weichselbaum, R.R., Ishwaran, H., Yoon, T., Nuyten, D.S., Baker, S.W., Khodarev, N., Su, A.W., Shaikh, A.Y., Roach, P., Kreike, B., Roizman, B., Bergh, J., Pawitan, Y., van de Vijver, M.J., Minn, A.J., 2008. An interferon-related gene signature for DNA damage resistance is a predictive marker for chemotherapy and radiation for breast cancer. Proc Natl Acad Sci U S A 105, 18490-18495.

Wennier, S.T., Liu, J., Li, S., Rahman, M.M., Mona, M., McFadden, G., 2012. Myxoma virus sensitizes cancer cells to gemcitabine and is an effective oncolytic virotherapeutic in models of disseminated pancreatic cancer. Mol Ther 20, 759-768.

Wertz, G.W., Moudy, R., Ball, L.A., 2002. Adding genes to the RNA genome of vesicular stomatitis virus: positional effects on stability of expression. J Virol 76, 7642-7650.

Wollmann, G., Rogulin, V., Simon, I., Rose, J.K., van den Pol, A.N., 2010. Some Attenuated Variants of Vesicular Stomatitis Virus Show Enhanced Oncolytic Activity against Human Glioblastoma Cells relative to Normal Brain Cells ▿ , J Virol, pp. 1563-1573.

Wong, W., Raufi, A.G., Safyan, R.A., Bates, S.E., Manji, G.A., 2020. BRCA Mutations in Pancreas Cancer: Spectrum, Current Management, Challenges and Future Prospects. Cancer Manag Res 12, 2731-2742.

Wu, Y., Mou, X., Wang, S., Liu, X.E., Sun, X., 2017. ING4 expressing oncolytic vaccinia virus promotes anti-tumor efficiency and synergizes with gemcitabine in pancreatic cancer. Oncotarget 8, 82728-82739.

Yachida, S., White, C.M., Naito, Y., Zhong, Y., Brosnan, J.A., Macgregor-Das, A.M., Morgan, R.A., Saunders, T., Laheru, D.A., Herman, J.M., Hruban, R.H., Klein, A.P., Jones, S., Velculescu, V., Wolfgang, C.L., Iacobuzio-Donahue, C.A., 2012. Clinical significance of the genetic landscape of pancreatic cancer and implications for identification of potential long-term survivors. Clin Cancer Res 18, 6339-6347.

Yu, D., Jin, C., Ramachandran, M., Xu, J., Nilsson, B., Korsgren, O., Le Blanc, K., Uhrbom, L., Forsberg-Nilsson, K., Westermark, B., Adamson, R., Maitland, N., Fan, X., Essand, M., 2013. Adenovirus serotype 5 vectors with Tat-PTD modified hexon and serotype 35 fiber show greatly enhanced transduction capacity of primary cell cultures. PLoS One 8, e54952.

Zeng, S., Pottler, M., Lan, B., Grutzmann, R., Pilarsky, C., Yang, H., 2019. Chemoresistance in Pancreatic Cancer. Int J Mol Sci 20.

Zhang, K.X., Matsui, Y., Hadaschik, B.A., Lee, C., Jia, W., Bell, J.C., Fazli, L., So, A.I., Rennie, P.S., 2010. Down-regulation of type I interferon receptor sensitizes bladder cancer cells to vesicular stomatitis virus-induced cell death. Int J Cancer 127, 830-838.

Zhang, Y.A., Nemunaitis, J., Samuel, S.K., Chen, P., Shen, Y., Tong, A.W., 2006. Antitumor activity of an oncolytic adenovirus-delivered oncogene small interfering RNA. Cancer Res 66, 9736-9743.

Zhang, Z., Han, H., Rong, Y., Zhu, K., Zhu, Z., Tang, Z., Xiong, C., Tao, J., 2018. Hypoxia potentiates gemcitabine-induced stemness in pancreatic cancer cells through AKT/Notch1 signaling. J Exp Clin Cancer Res 37, 291.

Zou, S., Sun, D., Liang, Y., 2017. The Roles of the SNARE Protein Sed5 in Autophagy in Saccharomyces cerevisiae, Mol Cells, pp. 643-654.